이학석사 학위논문

형광 리포터 마우스를 활용한 T 세포 소진 과정에 대한 연구

Study on the process of T cell exhaustion using fluorescent reporter mice

울 산 대 학 교 대 학 원

의 과 학 과

원 주 영

Study on the process of T cell exhaustion using fluorescent reporter mice

지 도 교 수 진 형 승

이 논문을 이학석사학위 논문으로 제출함

2024 년 8 월

울 산 대 학 교 대 학 원

의 과 학 과

원 주 영

원주영의 이학석사학위 논문을 인준함

심사위원 송영섭 (인)

심사위원 백인정 (인)

심사위원 진형승 (인)

울 산 대 학 교 대 학 원

2024 년 8 월

ABSTRACTS

CD8+ T cells are essential for fighting chronic viral infections and cancer. However, constant exposure to antigens and environmental cues in these conditions can lead to a dysfunctional or "exhausted" state in CD8+ T cells. Preventing this exhaustion is crucial for effective disease control. Immune checkpoint blockade (ICB) therapies, which inhibit receptors on these dysfunctional cells, have significantly improved anti-tumor and anti-viral responses. However, its lasting clinical benefits for many patients remain elusive. Understanding the cellular and molecular mechanisms underpinning the process of T cell exhaustion and ICB responses is crucial. Stem-like CD8+ T cells, governed by T cell factor 1 (TCF1), are essential for the response to ICB therapy. However, recent findings suggest that the reliance on TCF1+CD8+ T cells for ICB efficacy may vary across different tumor contexts. The transcription factor TOX regulates genetic programs that initiate and maintain T cell exhaustion.

To explore the factors influencing the differentiation or exhaustion of CD8+ T cells within tumors, the expression dynamics of TCF1 and TOX in CD8+ T cells were analyzed using a newly developed fluorescence reporter mouse capable of tracking TCF1 and TOX expression. Additionally, to evaluate the impact of PD-1 deficiency, a reporter mouse that lacks PD-1 expression was generated. Tumor growth and the expression levels of TCF1 and TOX in tumor-infiltrating lymphocytes (TILs) were examined in both LLC1 and LLC1-mOVA tumors implanted into these reporter mice.

Partial tumor control was observed in reporter mice implanted with LLC-mOVA, indicating a significant increase in TCF1 and TOX double-positive cells among CD8+ TILs compared to those in LLC1. This suggests that the dominance of the TCF1+TOX- population in CD8+ TILs within LLC1 reflects a naive-like status due to low antigen expression. In scenarios where cancer antigenicity remained unchanged, inhibiting PD-1 had minimal effect on tumor control or TCF1 and TOX expression dynamics. However, when both increased antigenicity and PD-1 deficiency were present, notable differences were observed in tumor control and the differentiation of CD8+ TILs. CD8+ TILs from PD-1 KO mice with LLC1-mOVA exhibited a majority of TCF1-negative populations undergoing progressive differentiation into effector-like transitory cells, characterized by the TCF1-TOX+ population. Expression levels of Tim-3, 4-1BB, CD226, and granzyme B significantly increased in the TCF1-negative population of CD8+ TILs, with higher levels observed in the TCF1-TOX- population compared to the TCF1-TOX+ late dysfunctional population. This study employed a reporter mouse model to visualize TCF1 and TOX expression, correlating these dynamics with tumor immunogenicity

and elucidating the relationship between optimal CD8+ TIL priming, differentiation, and tumor factors, thus enhancing the understanding of ICB therapy efficacy.

CONTENTS

LIST OF FIGURES

ABBREVIATIONS

TCF1: T cell factor 1

TOX: Thymocyte selection-associated high mobility group box protein

CTL: cytotoxic T cell

TME: tumor microenvironment

UTR: Untranslated Region

APC: Antigen presenting cell

MHC: Major Histocompatibility Complex

TAA: tumor-associated antigen

CTLA-4: Cytotoxic T-lymphocyte associated protein 4

PD-1: Programmed cell death receptor-1

PD-L1: Programmed Cell Death Ligand-1

TIM-3: T cell immunoglobulin-3

LAG-3: Lymphocyte activation gene-3

TIGIT: T cell immunoglobulin and ITIM domain

ICI: Immune checkpoint inhibitor

ICB: Immune checkpoint blockade

FOXO1: Forkhead box protein O1

TIL: Tumor-infiltrating lymphocyte

TST: tumor-specific T

IFN-g: Interferon gamma

CRISPR: clustered regularly interspaced short palindromic repeats

KO: knockout

MFI: Median fluorescence intensities

Tex: exhausted T cell

Tpex: precursor exhausted T cell

Ttex: terminal exhausted T cell

Tn: naïve T cell

Tcm: central memory T cell

Tem: effector memory T cell

Teff: effector T cell

1. Introduction

1.1. Cancer immunotherapy and immunogenicity

Cancer immunotherapy, which has emerged as a promising treatment, utilizes the immune system to combat cancer [1]. This therapy aims to stimulate strongly the immune system by increasing the presentation of tumor antigens to cytotoxic T cells or introducing novel anti-tumor properties to immune cells, with the goal of effectively fighting cancer cells [2]. Traditional chemotherapy continues to be the primary standard of care for cancer treatment and provides therapeutic benefits. Nevertheless, it is accompanied by adverse effects stemming from its non-selective cytotoxicity towards healthy cells. Furthermore, chemotherapy can weaken the immune system and, in certain instances, may lead to secondary carcinogenesis and cancer recurrence post-treatment. In contrast, cancer immunotherapy aims to modulate the immune system to selectively target neoplastic cells [3]. Immunotherapy has revolutionized cancer treatment over the past decade by promoting anti-tumor immune responses in patients across various types of tumors, inducing significant and sustained responses [4].

Cancer immunotherapy relies on enhancing robust cytotoxic T cell (CTL) responses against tumor-associated antigens (TAAs), a capability referred to as "immunogenicity." Cancer cells possess immunogenicity. The outcomes of cancer immunotherapy vary depending on the immunogenicity of the cancer [5]. Cancer cells accumulate mutations, including uncontrolled proliferation, genetic instability, and altered protein expression. Mutated self-proteins expressed by cancer cells impart immunogenicity, enabling the immune system to recognize and eliminate them. Various TAAs have been identified over the years. Examples include tyrosinase, CEA, NY-ESO-1, MART-1, among others [6-12]. Recent research has demonstrated a correlation between the increased immunogenicity induced by membrane-localized antigens (mAgs) and improved patient survival rates and responsiveness to immune checkpoint inhibitors (ICIs) across various cancer types [13].

Cytotoxic T cells are essential for targeting and eliminating infected or transformed cells in the body. Antigen-presenting cells (APCs) process antigens into antigenic peptides, which are then loaded onto MHC molecules. These peptide-MHC complexes are presented to T cells, which recognize specific antigenic peptides presented on the surface of APCs through their T cell receptors (TCRs) [14]. The extensive formation of large populations of TAA-specific cytotoxic T cells is crucial for preventing cancer evasion. When the number of TAA-specific T cells attacking cancer is limited, immunological editing occurs, allowing poorly immunogenic cancer cells to survive and proliferate. Conversely,

through immunotherapy, the expansion of a large pool of cytotoxic CD8 T cells specific to TAAs leads to the destruction of more cancer cells, thereby reducing the likelihood of immunological editing and cancer evasion [2]. T cells require additional signals from APCs for effective activation. These signals can be either stimulatory or inhibitory and regulate the degree of T cell activation. Stimulatory co-stimulation occurs through interactions such as the CD80-CD28 binding, while inhibitory interactions involve molecules like CTLA-4 and PD-L1 with PD1. The balance between positive and negative co-stimulation determines the degree of T cell activation [14-16]. Recently, immunotherapy using immune checkpoint inhibitors (ICIs) that block immune checkpoints such as CTLA-4, PD-1 and PD-L1 to control inhibitory interactions has been employed. This approach demonstrates efficacy across various cancer treatments by sustaining immune responses against cancer to promote its eradication. However, unfortunately, only a portion of patients shows consistent clinical benefits [5]. To overcome these challenges, research on stimulating the immune system to enhance anti-tumor immunity, along with investigating biomarkers for predicting treatment responses in patients, appears necessary [2, 17].

1.2. PD-1/PD-L1 axis in the regulation of immune cell functions

Cancer can evade immune surveillance by attenuating the function of cytotoxic T cells, which is achieved by weakening the efficacy of immune-suppressive cells. According to existing studies, such evasion mechanisms are known to be particularly induced by various immune-suppressive proteins produced by non-tumor cells, immune cells and epithelial cells, present in tumor cells or the tumor microenvironment (TME) [3].

Overexpression of PD-1(Programmed Cell Death Protein-1) and PD-L1(Programmed Cell Death Ligand-1) leads to immune suppression in most cancers and inflammatory processes [3]. PD-1 is expressed on the surface of various cells, including T cells and precursor B cells. It plays crucial role in regulating the immune response to human cells, functioning to suppress the immune system and enhance self-tolerance by inhibiting the activity of cytotoxic T cells [18]. This protein serves to limit autoimmune diseases but also has the potential to impede the immune system's ability to eradicate cancer cells [19, 20]. PD-L1 expression has been identified in diverse types of tumor cells, with both mouse and human tumor cells showing an increase in PD-L1 levels upon IFN-g stimulation [21]. When PD-L1 on the surface of tumor cells interacts with the PD-1 on T cells, it induces the deactivation of cytotoxic T cells, which subsequently send inhibitory signals to immune cells to switch off. Consequently, T cell deactivation ensues, leading to immune tolerance. Such immune tolerance can impede the interaction between T cells and MHC and hinder immune responses [3, 22].

Research in PD-1 Knock-Out (KO) mice indicates that PD-1 plays a negative regulatory role in immune responses. Various types of PD-1 KO mice exhibit splenomegaly or hepatomegaly. Studies also show symptoms of lupus-like proliferative arthritis and glomerulonephritis, or induction of cardiomegaly and cardiomyopathy [23]. PD-1 deficient 129/SV mice exhibited moderate splenomegaly, characterized by an increase in cell density in lymphoid and bone marrow compartments. Furthermore, there was an increased proliferative response of B cells to anti-IgM antibodies, along with a selective increase in serum IgG3 levels and specific IgG3 antibody responses to T-cell-independent(TI-2) antigens. Concurrently, a notable decrease in CD5 expression was observed in the peritoneal B-1 cell population of PD-1 deficient mice [24]. Therefore, it has been proposed that PD-1 is engaged in the negative regulation of certain facets of B cell activity, such as class switching [24]. Aged C57BL/6(B6)-PD-1 KO congenic mice exhibited characteristic lupus-like proliferative arthritis and glomerulonephritis, with observed glomerulonephritis showing predominant IgG3 deposition [25]. PD-1 KO mice with the disease showed bulging of the eyes a few weeks before death, and upon autopsy, all afflicted mice displayed significantly enlarged hearts and various degrees of liver enlargement [26]. When propagated on a BALB/c background, PD-1 KO mice commenced premature mortality from the age of 5 weeks onwards. By the age of 30 weeks, two-thirds of the PD-1 deficient mice had succumbed, whereas all of the PD-1-competent control counterparts remained viable. Conversely, premature mortality was not observed in B6-PD-1-/- mice [26]. The phenotype of PD-1 KO mice is more pronounced in mice with autoimmune susceptibility. NOD mice, predisposed to spontaneous type 1 diabetes, null mutations of PD-1 or its ligands expedited the activation of T cells responsive to blood glucose levels, leading to markedly increased infiltration, earlier onset of diabetes, and more severe progression compared to PD-1-competent counterparts [27]. PD-1 deficient MRL mice exhibit severe myocarditis and pneumonia, with over 70% of the mice succumbing within 10 weeks of age. An intriguing observation is that PD-1 sufficient MRL mice do not exhibit myocarditis. This finding suggests that the PD-1 null genotype elicits unrecognized host autoimmune predisposition [27].

1.3. T cell exhaustion, TCF1 and TOX

“T cell exhaustion" is a comprehensive term employed to characterize the T cell reaction to persistent antigenic stimulation. "Exhaustion" typically refers to effector T cells with diminished ability to secrete cytokines and upregulated expression of inhibitory receptors [28]. Initially identified in the context of chronic viral infections, it has recently been observed in responses to tumors as well [29]. Long-term antigen stimulation induces T cell dysfunction/exhaustion [30].

Generally, compared to effector or memory T cells, exhausted T cells exhibit altered or diminished effector functions. Functionally, they show gradual decreases in cytokine production, proliferative capacity, polyfunctionality, and cytotoxicity [31], while phenotypically expressing high levels of various inhibitory receptors such as PD1, CTLA-4, TIM3, LAG3 and TIGIT. Transcriptionally, factors associated with exhaustion and memory formation, such as TCF, TOX, T-bet, Eomes, and FOXO1, each undergo changes. These functional, phenotypic, and transcriptional alterations are apparent in both in vitro and in vivo models [30, 32].

Many researchers tend to assess exhausted T cells solely based on the expression of inhibitory receptors. However, this is not a definitive characteristic of exhausted states since many functionally competent effector T cells also express inhibitory receptors [29]. Recent studies have revealed the presence of two distinct subpopulations within exhausted T cells. The first is a precursor (or progenitor) subset, often referred to as stem-like or memory-like, and the second is a terminally differentiated subset [29]. Precursor exhausted CD8+ T cells undergo self-renewal and differentiate into terminally exhausted CD8+ T cells, the latter exhibiting decreased effector functions. Direct comparison of these subsets has shown that precursor exhausted CD8+ T cells express fewer immune inhibitory receptors (IRs) and more frequently express specific transcription factors such as T cell factor 1(TCF) [33].

TCF1 derived from the TCF7 gene, is pivotal in the development and differentiation of T cells. TCF1 is dynamically regulated, being down-regulated in effector T cells and partially restored in memory T cells. Furthermore, it regulates the differentiation and maintenance of exhausted CD8+ T cells in chronic infections and tumors, as well as the differentiation and longevity of memory CD8+ T cells [34-37]. In the early stages of chronic infections and tumors, exhausted T cells are defined as precursor exhausted T cells (Tpex) or terminal exhausted T cells (Ttex) based on the expression levels of TCF [34]. TCF+ T cells chronically stimulated are considered to possess stem cell-like properties in some subsets, resembling memory T cell populations [29]. Similar to memory or stem cells, they exhibit long-term survival and self-renewal capabilities, as well as proliferative potential. However, unlike conventional memory T cells, these TCF+ T cells exhibit inhibitory receptors, including PD-1 and undergo

continuous differentiation into terminally exhausted effector T cells. These TCF+ exhausted T cells are classified as precursor exhausted T cells. They constitute specific subsets within the tumor-infiltrating lymphocytes (TILs) of CD8+ tumors, sustaining long-term immune responses mediated by CD8+ T cells [38-40].

Because TCF1 expression is known to play a role in maintaining stemness in hematopoietic stem cells, many studies are underway to elucidate its role in the PD-$1^{lo/hi}$ Tex progenitor and progeny relationship. In $Tcf7^{-/-}$ mice, PD-$1^{lo/hi}$ CD8+ Tex cells fail to develop and cannot transition into exhausted cell lineages. Conversely, overexpression of the Tcf7 gene stabilizes PD-1lo stem-like cells and induces more sustained CD8+ T cell responses in a melanoma model. This demonstrates the crucial role of TCF1 in the differentiation of Tex cells [40]. Highly expressed TCF+ PD-1+ precursor cells exhibit strong proliferative and differentiation capabilities into terminal Tex cells, and they can survive even in the absence of antigens. TCF1− TILs show lower levels of PD-1 expression compared to TCF1+ CD8+ TILs, and terminally exhausted Tex cells with low TCF expression exhibit stronger cytotoxicity but shorter survival. Therefore, TCF+ PD-1+ CD8+ TILs with characteristics akin to stem cells and memory cells continuously infiltrate tumors, exerting high cytotoxicity through self-renewal and differentiation into terminal exhausted CD8+ TILs, thereby mediating tumor control and sustaining long-term immune responses [41, 42].

In the mouse B16-gp33 melanoma model, TCF1+ TILs expressed not only CXCR5, Ly108 (Slamf6), and CD62L but also memory markers such as PD-1, CTLA-4, and Lag3 [42]. The expression of these checkpoint molecules suggests that this subset may be an important target for anti-PD1 and anti-CTLA-4 therapies. Indeed, upon adoptive transfer, gp33-specific TCF1+ TILs were able to expand and differentiate into TCF1− cells while maintaining secretion of IL-2 and TNF-α. Similarly, TCF1+PD-1+CD8+ T cells found in chronic infections exhibited proliferative capacity and sustained the TCF1+ cell population while continuously producing TCF1−PD-1+CD8+ T cells [38]. Furthermore, the sustained anti-tumor effects of anti-PD1 and anti-CTLA-4 therapies in mice depended on Tcf7 expression in T cells [42]. Several studies emphasize a dichotomy between terminally differentiated exhausted T cells as TCF1- and the self-renewing TCF1+ cell population derived from them. However, the developmental relationship between these subsets is not yet fully understood [29].

The expression of the transcription factor TOX (Thymocyte selection-associated high mobility group box protein) is associated with CD8+ T cell exhaustion and TCF. While TCF maintains the response of fatigued CD8+ T cells, TOX is essential for the transcriptional reprogramming and survival of exhausted CD8+ T cells. Recent studies have mapped the expression of TCF and TOX in human

CD8+ T cells to their functional differentiation and specificity. They revealed that while TCF is generally expressed in naive CD8+ T cells and early differentiated memory cells, TOX is expressed in the majority of effector memory CD8+ T cells [33, 34].

TOX expression is promoted by NFAT transcription factors following T cell activation. In infiltrating CD8+ T cells within tumors from human melanoma and non-small cell lung cancer (NSCLC) samples, TOX exhibited increased expression in CD8+ T cells showing high expression of PD-1. It plays an pivotal role in T cell development and has recently garnered attention for its involvement in inducing T cell exhaustion. Sustained expression of TOX induces exhaustion, as fatigue was not induced in the absence of TOX [43, 44].

When TOX is deleted in tumor-specific T (TST) cells, the chromatin of inhibitory receptors such as Pdcd1, Entpd1, Havcr2, Cd244, and Tigit remains largely inaccessible, leading to their unaltered expression levels, while the expression of transcription factors like TCF is elevated. TOX-deleted TST cells exhibit a normal 'non-exhausted' immune phenotype but still have functional impairments. This suggests that the regulation of inhibitory receptor expression is dissociated from the loss of effector function [45]. TOX-deleted TST cells fail to persist within the tumor, indicating that the exhaustion program induced by TOX prevents excessive stimulation and activation-induced cell death of T cells in chronic antigen-stimulated environments like cancer [45].

Recent studies have demonstrated that TOX distinguishes exhausted CD8+ T cells from memory CD8+ T cells in various mouse models. These studies have shown that TOX is absolutely necessary for the transcriptional reprogramming and survival of exhausted CD8+ T cells [33]. Sustained high expression of TOX promotes the development of Tex cells by inducing continuous stimulation that alters transcriptional characteristics and epigenetic programs [43]. T cells with low expression of TOX/T-bet are found in an intermediate subset of exhausted T cells, and as the expression of TOX/T-bet in T cells begins to increase continuously, it induces changes in chromosomal recombination and RNA transcription, inhibiting differentiation into effector T cells and leading to entry into a state of exhaustion [46, 47].

TOX has been shown to act as a key transcriptional regulator in exhausted T cells while also playing a role in the persistence of T cells during chronic infections and cancer [43, 48]. TOX is necessary for the persistence of CD8+ T cells, resembling precursor cells, but TOX-induced exhaustion of CD8+ T cells impairs the anti-tumor function of CD8+ TILs and hinders responsiveness to anti-PD-1 therapy [49]. In bladder cancer, it has been reported that inhibitory receptors of exhausted TILs expressing TOX can be reactivated. Additionally, TOX has been proposed as an immune biomarker and a significant

target for immunotherapy in hematologic malignancies. Recent studies have emphasized the significant role of the transcriptional regulator TOX in inducing the epigenetic reinforcement of exhaustion [47, 49]. However, important questions remain regarding the potential reversal of exhaustion's epigenetic program and how this could impact the persistence of T cell populations [29].

2. Materials and Methods

2.1. Mice

Genomic DNA was obtained from ear tissue using the Quick-DNA™ Miniprep Plus Kit (Zymo Research) according to the manual instructions. Tcf7-tdTomato knock-in reporter mouse were genotyped using primers TCF7-LH-for-#2 (5′-CCGTTCCTTCCGATGACAGT-3′) and TCF7-RH-#2-rev (5′-CCATGGGAGCTGGTCATGTT-3′) under the following protocol: 95°C for 5 min; 35 cycles of 95°C for 1 min, 62°C for 30 sec, and 72°C for 1 min 30 sec; final extension step at 72°C for 5 min. This method allows obtaining a 304 bp for the WT allele and a 1798 bp for the mutant allele. TOX-TagBFP knock-in reporter mouse were genotyped using primers TOX-F2 (5′-CCTCATGTCCAGGAAGGC-3′) and TOX-R2 (5′-TGGTCCACACTTCCTTCTGG-3′), followed by touch-down PCR—The process consists of two phases: Phase 1 involves incubation at 95°C for 3 min; 10 cycles of 95°C for 45 sec, 65°C for 45 sec (with a decrease of 0.5°C per cycle), and extension at 68°C for 1 min. This is followed by Phase 2, which includes 94°C for 45 sec; 39 cycles of 60°C for 45 sec, 70°C for 30 sec; final extension step at 72°C for 5 min. This method allows obtaining a 556 bp for the WT allele and a 1268 bp for the mutant allele. PD-1 knockout (KO) mice were genotyped using primers PD-1 KO-for (5'-GGGGAGGAGGAAGAGGAGAC-3'), PD-1 KO-rev (5'-ATAGGAACCGAGGGTGAACG-3'). This method allows obtaining a 213 bp for the WT allele and a 196 bp for the mutant allele, followed by touch-down PCR. PCR products were resolved by electrophoresis on a 1.5% agarose gel. Mice homozygous for both reporters (Tcf7-tdTomato/TOX-TagBFP) were used in experiments. Tcf7-tdTomato/TOX-TagBFP mice were bred with PD-1 KO mice to produce Tcf7-tdTomato/TOX-TagBFP /PD-1 KO mice. Mouse strains were bred and maintained in the SPF animal facility of the Asan Medical Institute of Convergence Science and Technology (AMIST).

2.2. DNA plasmids

To generate the LLC1 cell line, we cloned the membrane-bound ovalbumin (mOVA) into a bicistronic GFP expression vector, pSBbi-GN (Addgene plasmid no. 60517). The mOVA regions were PCR amplified from the Addgene plasmids—pCI-neo-mOVA (plasmid no. 25099)—and ligated into the Sfi1 restriction sites of the GFP vector.

2.3. Cell lines

LLC1 (CRL-1642) lung carcinoma was purchased from the American Type Culture Collection (ATCC). LLC1 cells were transfected with the plasmid pSBbi-GN expressing mOVA and T7-SB100 (Plasmid #34879) using the Neon Transfection System (Invitrogen). After transfection, we sorted the GFP-positive cells using the FACSAria cell sorter (BD Biosciences).

2.4. Cell culture

All cells lines were cultured in DMEM medium supplemented with 10% heated-inactivated FBS (Welgene), 1x Antibiotic-Antimycotic Solution(Welgene), 10mM HEPES(Welgene) at 37°C in 5% CO2.

2.5. Mouse tumor model

LLC1 cell lines cultured in the log phase were harvested and suspended in Hank's Balanced Salt Solution (HBSS, Welgene). Subsequently, 100 μl of cell suspension containing 2.5 × 10^6 cells were injected subcutaneously into the pre-shaved flank of mice under anesthesia induced by 2% gaseous isoflurane. Tumor size was periodically assessed using a digital Vernier caliper, and the volume was determined in cubic millimeters using the formula V = 0.5 × a × b^2, where 'a' and 'b' denote the long and short diameters of the tumor, respectively. Tumor weight was measured at the conclusion of the experiment.

2.6. Tissue processing

Mouse tumors were chopped into small pieces and digested with collagenase IV (250 unit/ml, Worthington Biochemical Cooperation) and DNase I (100 μg/ml, Roche Diagnostics GmbH) in HBSS using a gentleMACS dissociator (Miltenyi Biotec). TILs were enriched using gradient centrifugation with HisepTM LMS 1084 (Himedia Laboratories), and single cells were subsequently recovered.

2.7. Immunophenotyping

Single cells were obtained by passing the spleen through a 70 um nylon cell strainer (SPL Life Sciences). Then RBCs were lysed using 1x RBC lysis buffer (BioLegend). The cells were seeded in a 24well plate at 1.2x10^6cells in complete R10 medium comprising 10% heat-inactivated FBS (Welgene), 1x Antibiotic-Antimycotic Solution (Welgene), 25mM HEPES (Welgene), 1mM sodium Pyruvate (Welgene), 1x MEM (Welgene), 2mM L-Glutamine (Welgene), and 50μM 2-mercaptoethanol

(Sigma) in RPMI-1640 (Welgene). The cells were stimulated under the following two conditions: either with Anti-CD3 5ug/ml (BioLegend) and anti-CD28 2.5ug/ml (BioLegend) in DPBS, or with 1ug/ml Concanavalin A (Sigma). All conditions included 1ug/ml human IL-2 (Peprotech). Cells were then analyzed by flow cytometry between day 1 and day 3 post-stimulation.

2.8. Flow cytometry

Mouse single cells were blocked with anti-mouse CD16/32 (BioLegend) after using Zombie NIR Fixable viability dye (BioLegend) to exclude dead cells. Then stained with with fluorochrome-conjugated antibodies in FACS buffer (DPBS containing 0.5% BSA and 0.1% NaN3) for 15 minutes at room temperature. Intracellular staining was conducted by fixing and permeabilizing cells with a Foxp3/Transcription Factor Staining Buffer kit (Tonbo Biosciences) according to the standard protocols. The following fluorochrome-conjugated anti-mouse antibodies were used : anti-CD3(17A2), anti-CD45(30-F11), anti-CD4 (GK1.5), anti-CD8 (53-6.7), anti-CD62L (MEL-14), anti-CD226(10E5), anti-CD137(17B5), anti-PD-1 (RMP1-30), anti-TIM3(RMT3-23), anti-CD44(IM7), anti-CD69(H1.2F3), anti-CD25(PC61), anti-CD19(6D5), anti-CD11b(M1/70), anti-CD11c(N418), anti-CD206(C068C2), anti-Ly6C(HK1.4), anti-Ly6G(1A8), anti-I-A/I-E(M5/114.15.2), anti-F4/80(T45-2342), anti-Foxp3(FJK-16s), anti-Ki-67(16A8), anti-Granzyme B(QA16A02). Flow cytometry was performed using an CytoFLEX flow cytometer (Beckman Coulter, Brea, CA) and FACS Canto II cytometer (BD Biosciences). Data were analyzed with FlowJo software (v.10.5.3, TreeStar)

3. Results

3.1. Generation of Tcf7-tdTomato/TOX-TagBFP reporter mice and their PD-1 deficient counterparts

TCF1 and TOX play fundamental roles in T cell development, stemness, and memory formation. In addition, TCF1 works with TOX to maintain exhausted T cells in tumors and chronic infections. Under conditions of chronic antigen stimulation, the expression of TCF1 and TOX changes dynamically across various T cell subsets. To delineate the heterogeneous expression of TCF1 and TOX in T cells under various inflammatory environments, a fluorescent reporter mouse capable of evaluating the expression of TCF1 and TOX through fluorescent expression was created.

First, the *Tcf7*-tdTomato knock-in reporter mouse line was created by inserting a P2A-tdTomato cassette into the 3'UTR of the Tcf7 locus on chromosome 11. A targeting construct was designed with a P2A-tdTomato knock-in cassette flanked by homology arms. Second, the TOX-TagBFP knock-in reporter mouse line was generated by inserting a P2A-TagBFP cassette into the 3'UTR of the TOX locus on chromosome 4. A double reporter strain was produced by breeding the Tcf7-tdTomato line with the TOX-TagBFP line. Mice homozygous for both reporters (Tcf7-tdTomato/TOX-TagBFP) were used in experiments and named "TT" mice. PCR-based genotyping revealed that the knock-in of the P2A-tdTomato cassette produced a PCR product size of 1789 bp, while the knock-in of the P2A-TagBFP cassette produced a PCR product size of 1268 bp **(Figure 1A and 1B)**. To assess the impact of PD-1 deficiency on the expression of TCF1 and TOX in T cells, TT mice were bred with *PDCD-1* knockout (KO) mice to produce TT PD-1 KO mice. The PD-1 KO mice were created using CRISPR/Cas9 genome editing to delete 17 nucleotides in exon 1 of the *PDCD1* gene on chromosome 1 **(Figure 2A)**. PCR-based genotyping showed that the 17 bp deletion in the PDCD1 gene produced a PCR product of 196 bp, compared to the wildtype mouse, which showed a product of 213 bp **(Figure 2B)**.

Since surface PD-1 is not expressed on resting T cells, mouse splenocytes were activated using anti-CD3/CD28 stimulation to induce surface PD-1 expression. FACS analysis revealed that PD-1 was expressed in T cells from TT mice, but not in T cells from TT PD-1 KO mice **(Figure 2C)**.

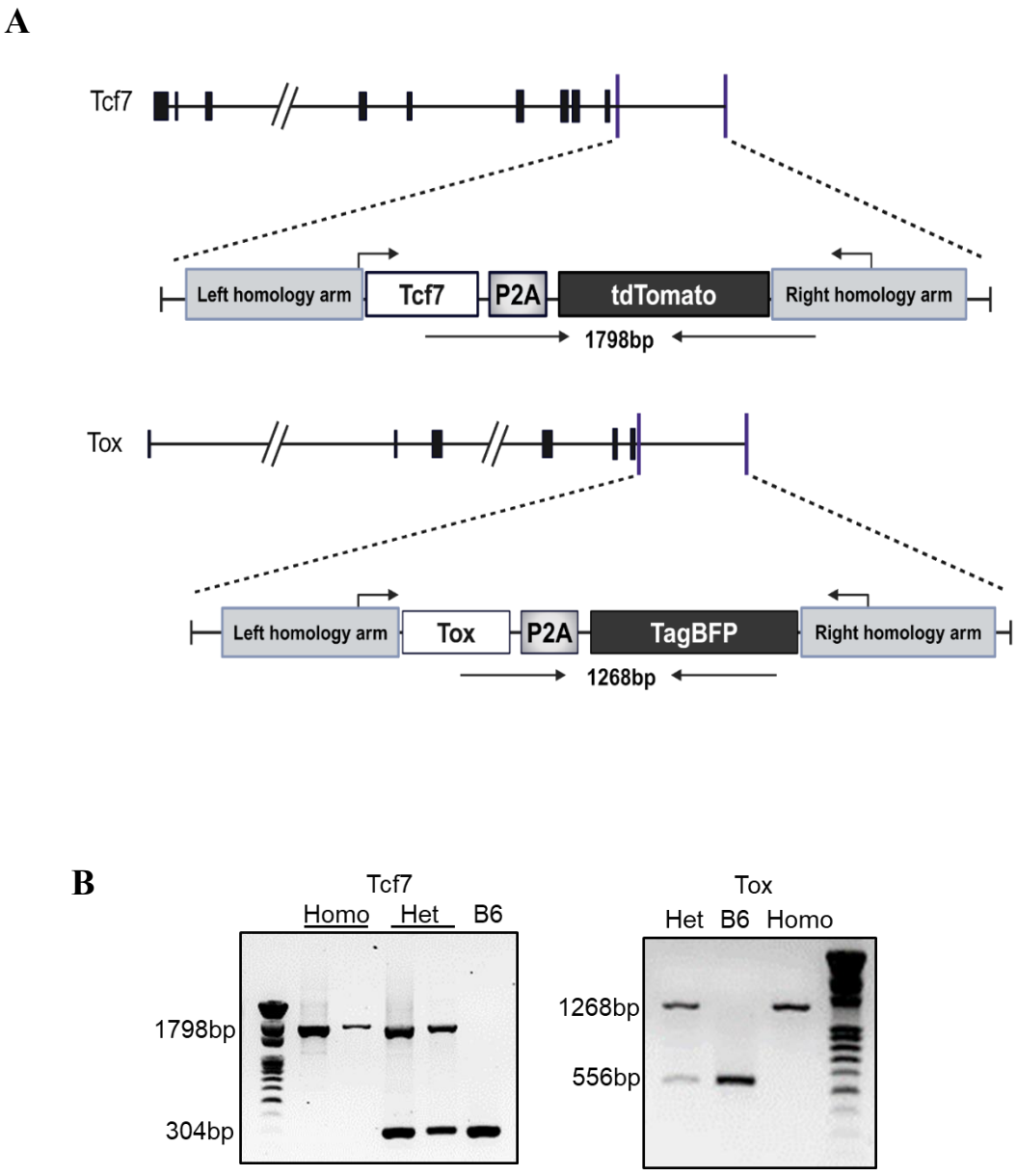

Figure 1 Generation of mice carrying both Tcf7-P2A-tdtomato and TOX-P2A-TagBFP

(A) A P2A-tdTomato cassette flanked by homology arms was inserted into the 3' UTR of the Tcf7 locus on chromosome 11. When TCF1 is expressed, tdTomato is co-expressed. A P2A-tagBFP cassette flanked by homology arms was inserted into the 3'UTR of the TOX locus on chromosome 4. When TOX is expressed, BFP is co-expressed. (B) gDNA was extracted from mouse ear tissue, and PCR was

conducted using the primers TCF7-LH-for-#2 (5′-CCGTTCCTTCCGATGACAGT-3′) and TCF7-RH-#2-rev (5′-CCATGGGAGCTGGTCATGTT-3′). The wild-type genotype displayed a band of 304 bp, while the P2A-tdTomato knock-in genotype was identified by a band of 1798 bp. To verify P2A-tagBFP, PCR was conducted using the primers TOX-F2 (5′-CCTCATGTCCAGGAAGGC-3′) and TOX-R2 (5′-TGGTCCACACTTCCTTCTGG-3′). The wild-type genotype displayed a band of 556 bp, while the BFP knock-in genotype was identified by a band of 1268 bp. The bands were separated by electrophoresis on a 1.5% agarose gel.

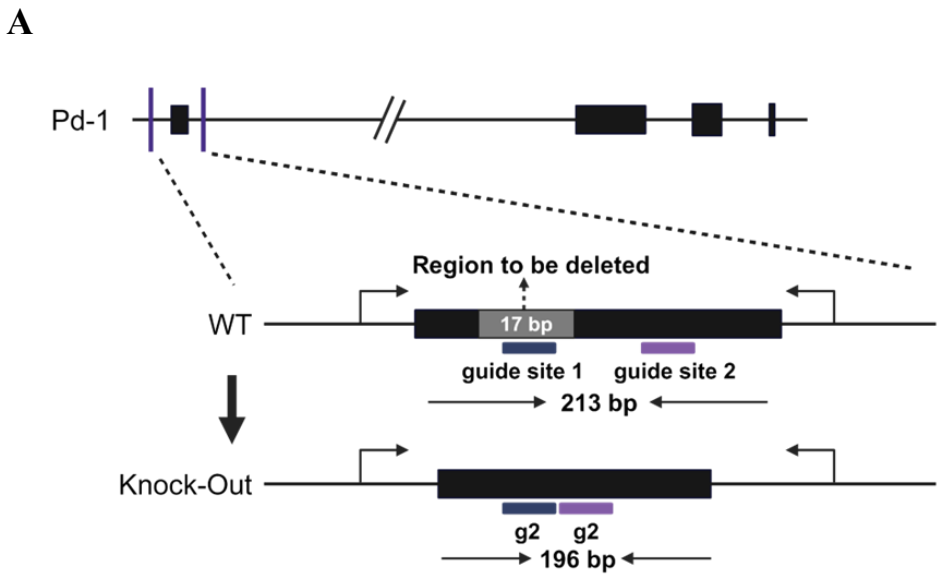

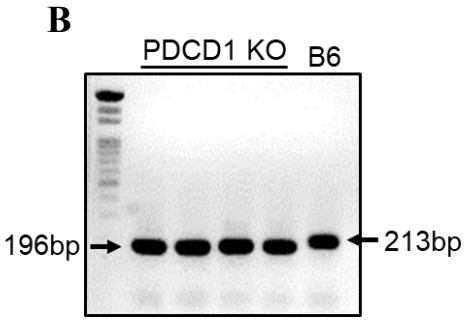

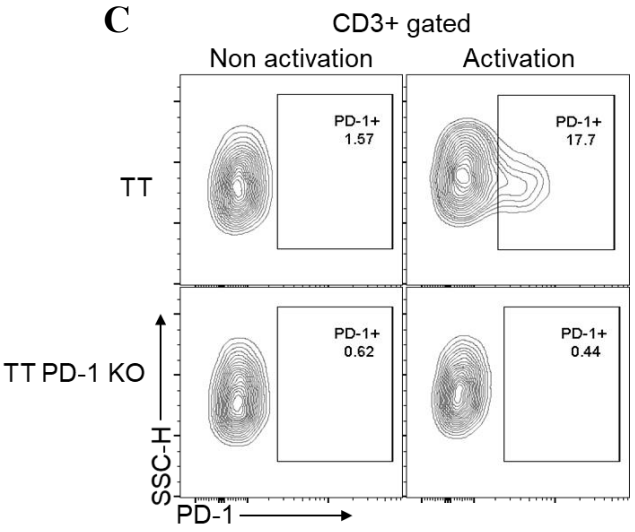

Figure 2 Generation of PDCD1 knockout mice carrying both Tcf7-P2A-tdtomato and TOX-P2A-TagBFP

(A Deletion of 17 nucleotides in exon 1 of the PDCD1 gene on chromosome 1 using CRISPR/Cas9 genome editing. (B) gDNA was extracted from mouse ear tissue, and PCR was conducted using the primers PD-1 KO-for (5'-GGGGAGGAGGAAGAGGAGAC-3'), PD-1 KO-rev (5'-ATAGGAACCGAGGGTGAACG-3'). Subsequently, The bands were separated by electrophoresis on a 1.5% agarose gel. The wild-type genotype displayed a band of 213 bp, while the PDCD1 knock-out genotype was identified by a band of 196 bp. (C) Splenocytes were stimulated to confirm PD-1 KO status by assessing PD-1 expression. Splenocytes from Tcf-tdTomato/TOX-BFP (TT) mice or Tcf-tdTomato/TOX-BFP/PD-1 KO (TT PD-1 KO) mice were cultured in medium on plates coated with anti-CD3 mAb and anti-CD28 mAb for 6 hours, followed by flow cytometry analysis.

3.2. TCF1 and TOX expression in CD8+ T cells is downregulated by TCR stimulation and accelerated by PD-1 deficiency

To investigate the kinetics of TCF1 and TOX expression induced by TCR stimulation, CD8+ T cells were isolated from the spleen and activated with anti-CD3 and anti-CD28 antibodies. Initially, TCF1 and TOX expression levels were measured across memory subsets in a steady state. Both TCF1 and TOX were highly expressed in naive T cells (Tn, CD62L+CD44-), with their expression progressively decreasing in the central memory (Tcm, CD62L+CD44+) and effector memory (Tem, CD62L-CD44+) subsets. In effector T cells (Teff, CD62L-CD44-), both TCF1 and TOX were expressed at high levels, similar to naive T cells **(Figure 3A and B)**.

After 24 hours of TCR stimulation (Day 1), most T cells were enriched for CD44+ memory T cells, and the expression of both TCF1 and TOX decreased. There was no difference in the frequency of TCF1+ or TOX+ T cells between the Tcm and Tem subsets. In both subsets, higher CD44 expression levels were associated with lower levels of TCF1 and TOX expression. After 48 hours (Day 2), there was an increase in the $TCF1^{int}$ population, indicating increased downregulation of TCF1, while TOX expression was downregulated in most memory T cells except for a small population expressing intermediate levels of TOX. After 72 hours of TCR stimulation (Day 3), TCF1 and TOX expression was almost undetectable in both Tcm and Tem subsets. This contrasts with the expression patterns observed in memory subsets at steady state, suggesting that TCR stimulation temporarily reduces TCF1 and TOX expression regardless of the T cell differentiation status **(Figure 3C)**.

To understand the correlation between PD-1 expression and TCF1 and TOX expression and its impact on T cell differentiation, CD8+ T cells isolated from PD-1 deficient TT mice were similarly stimulated and analyzed for TCF1 and TOX expression. In the steady state, the abrogation of PD-1 did not result in any changes in T cell differentiation or the expression of TCF1 and TOX **(Figure 3D)**. However, after 24 and 48 hours of TCR stimulation, PD-1 deficient CD8+ T cells showed increased downregulation of TCF1 and TOX compared with PD-1 competent CD8+ T cells **(Figure 3E)**. Considering that TCR stimulation induces TCF1 and TOX downregulation, this suggests that the absence of PD-1 might accelerate the downregulation of TCF1 and TOX due to increased T cell activation strength. Indeed, 72 hours after TCR stimulation, CD44 expression levels in PD-1 deficient T cells were observed to be lower compared to WT T cells, indicating increased differentiation into effector T cells due to strong TCR stimulation **(Figure 3D)**. The analysis of TCF1 and TOX expression in CD4+ T cells during TCR-mediated activation revealed a pattern almost identical to that in CD8+ T cells **(Figure 4A to E)**. Collectively, TCF1 and TOX expression in T cells progressively decreased

following TCR stimulation, and strong T cell activation induced by PD-1 deficiency promoted this downregulation.

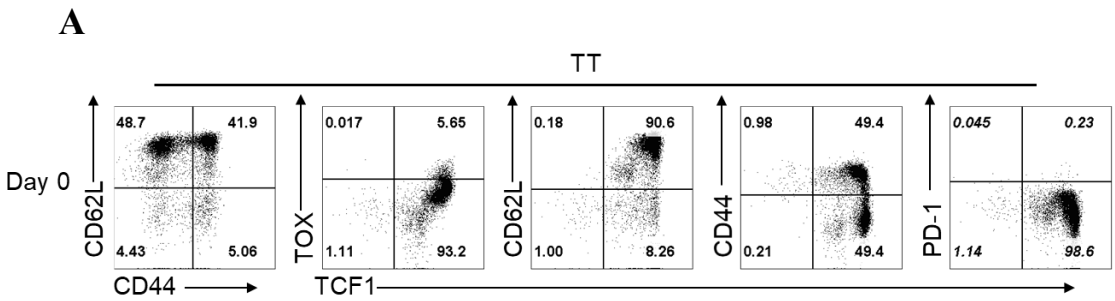

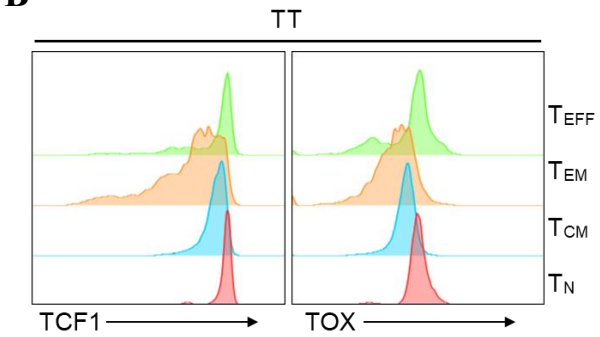

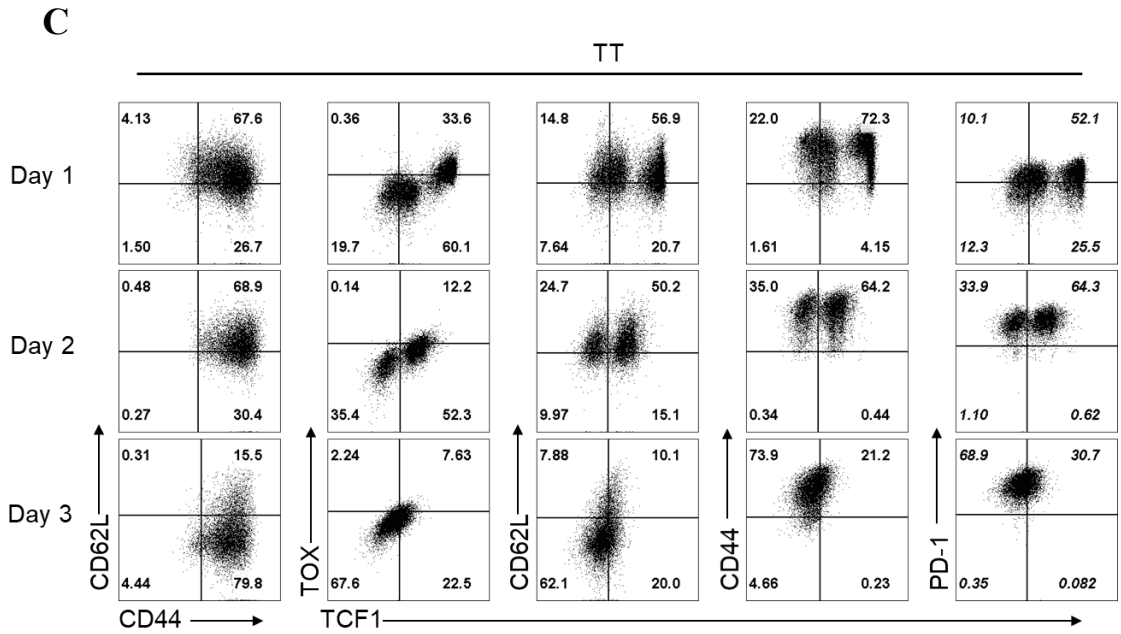

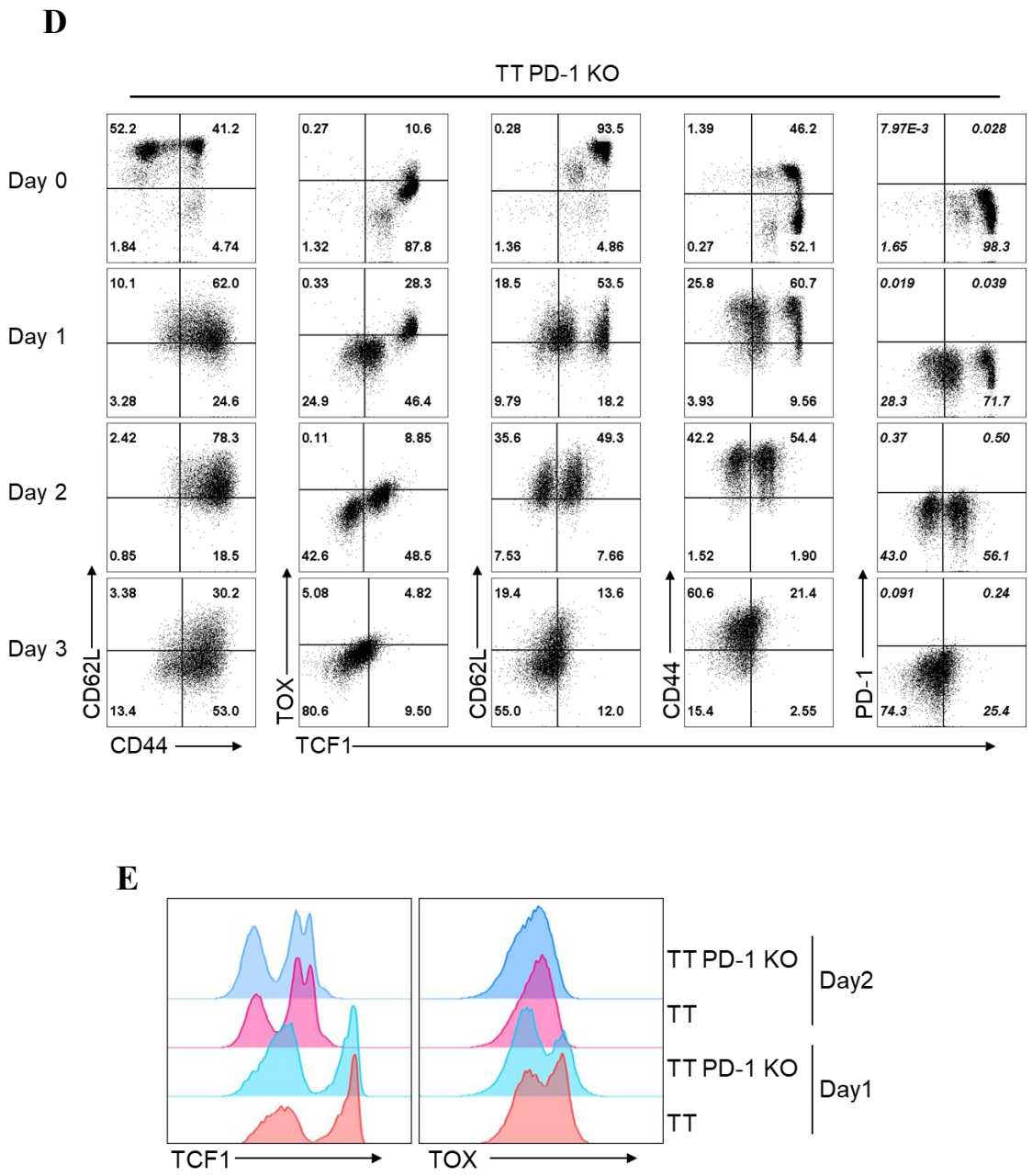

Figure 3 The change in TCF1 and TOX expression in CD8+ T cells stimulated with anti-CD3/CD28 in vitro

(A-E) Flow cytometry data showing the differentiation patterns of CD8+ T cells from splenocytes of TT or TT PD-1 KO mice stimulated with anti-CD3/CD28. Representative data also demonstrate the ability to monitor changes in TCF1 and TOX via fluorescence. T cells were identified by surface

expression of CD3. Subsequently, subsets within CD8+ T cells were distinguished. Naïve T cells were identified as CD62L+CD44+, while memory T cells were identified based on CD44 surface expression. Central memory T cells were identified as CD62L+CD44+, and effector memory T cells were identified as CD62L-CD44+. Effector T cells were identified as CD62L-CD44-.

(A) Flow cytometry data showing TCF1 and TOX expression levels across memory subsets of CD8+ T cells from TT mice under steady state. The data illustrate the differentiation patterns and the changes in TCF1 alongside variations in TOX, CD62L, CD44, and PD-1 within CD8+ T cells. (B) The histogram data showing TCF1 and TOX expression levels across memory subsets in a steady state. (C) Flow cytometry data showing the differentiation patterns and TCF1 and TOX expression of CD8+ T cells from splenocytes of TT mice stimulated with anti-CD3/CD28 from Day 1 to Day 3. The data illustrate the differentiation patterns and the changes in TCF1 alongside variations in TOX, CD62L, CD44, and PD-1 within CD8+ T cells. (D) Flow cytometry data showing the differentiation patterns and TCF1 and TOX expression of CD8+ T cells from splenocytes of TT PD-1 KO mice stimulated with anti-CD3/CD28 from Day 0(steady state) to Day 3. The data illustrate the differentiation patterns and the changes in TCF1 alongside variations in TOX, CD62L, CD44, and PD-1 within CD8+ T cells. (E) Histogram data comparing the expression levels of TCF1 and TOX between Day 1 and Day 2 post-stimulation in CD8+ T cells from two reporter mouse (TT and TT PD-1 KO) models.

A

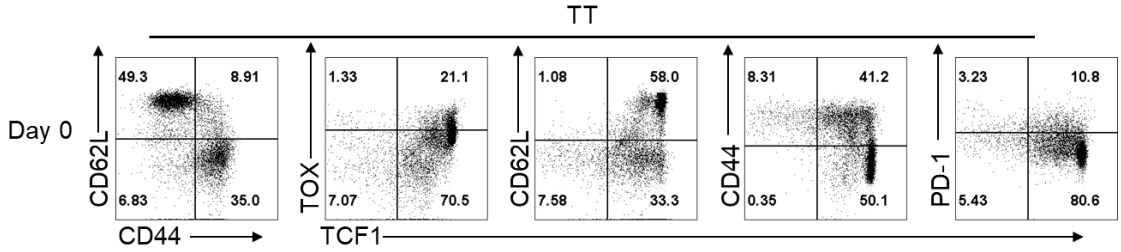

B

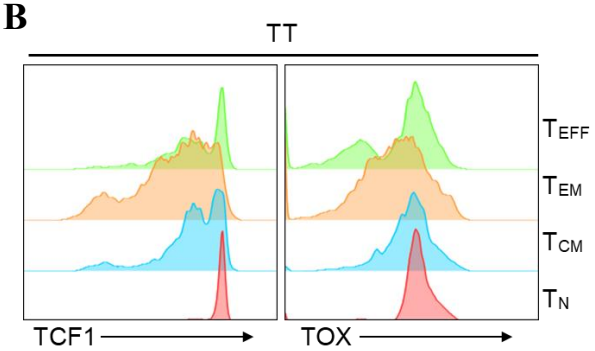

C

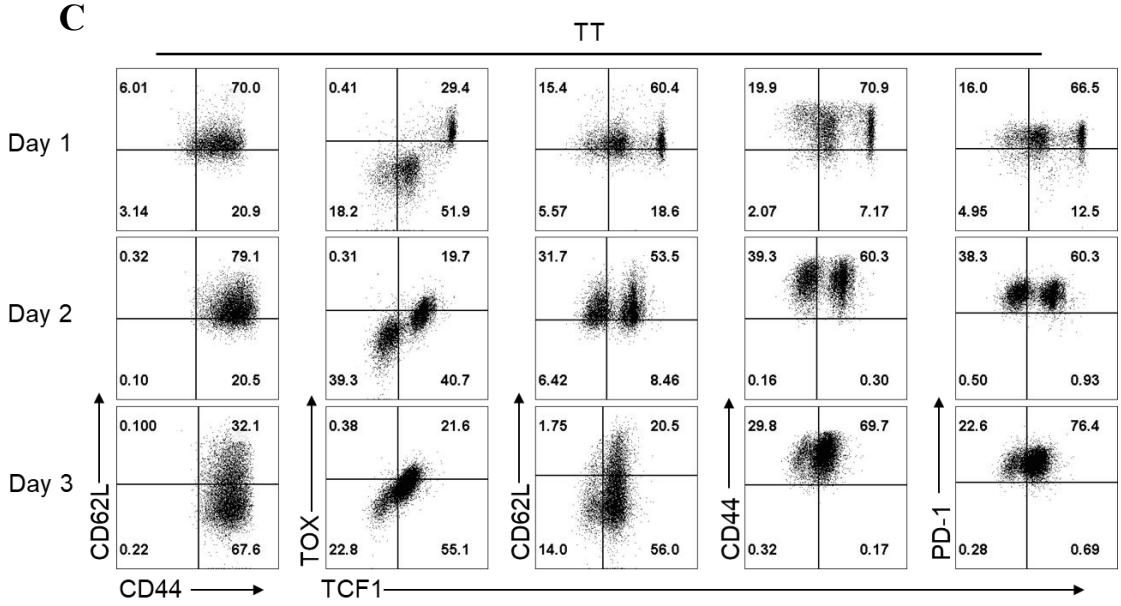

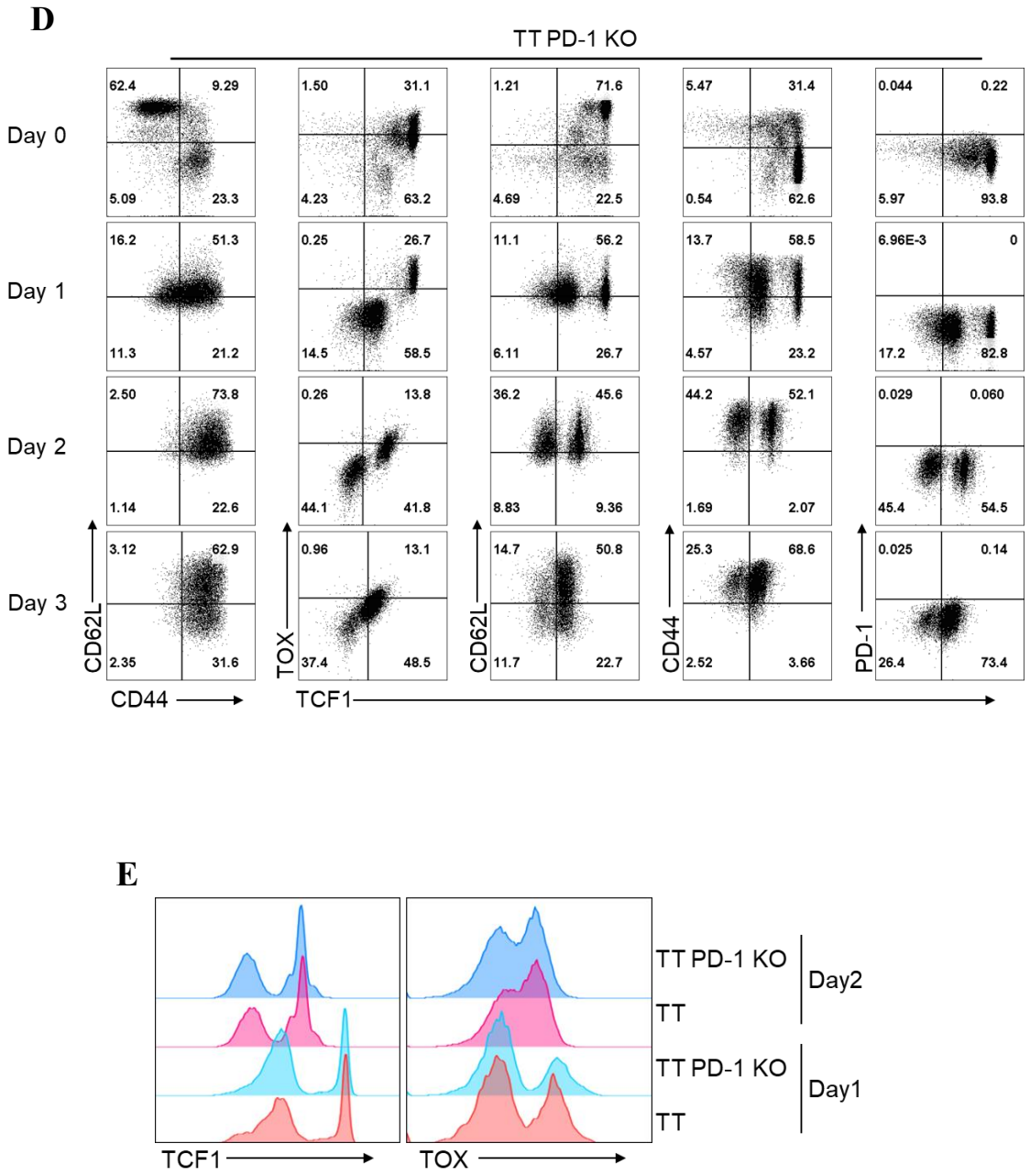

Figure 4 The change in TCF1 and TOX expression in CD4+ T cells stimulated with anti-CD3/CD28 in vitro

(A-E) Flow cytometry data showing the differentiation patterns of CD4+ T cells from splenocytes of TT or TT PD-1 KO mice stimulated with anti-CD3/CD28. Representative data also demonstrate the ability to monitor changes in TCF1 and TOX via fluorescence. T cells were identified by surface

expression of CD3. Subsequently, subsets within CD4+ T cells were distinguished. Naïve T cells were identified as CD62L+CD44+, while memory T cells were identified based on CD44 surface expression. Central memory T cells were identified as CD62L+CD44+, and effector memory T cells were identified as CD62L-CD44+. Effector T cells were identified as CD62L-CD44-.

(A) Flow cytometry data showing TCF1 and TOX expression levels across memory subsets of CD4+ T cells from TT mice under steady state. The data illustrate the differentiation patterns and the changes in TCF1 alongside variations in TOX, CD62L, CD44, and PD-1 within CD4+ T cells. (B) The histogram data showing TCF1 and TOX expression levels across memory subsets in a steady state. (C) Flow cytometry data showing the differentiation patterns and TCF1 and TOX expression of CD4+ T cells from splenocytes of TT mice stimulated with anti-CD3/CD28 from Day 1 to Day 3. The data illustrate the differentiation patterns and the changes in TCF1 alongside variations in TOX, CD62L, CD44, and PD-1 within CD8+ T cells. (D) Flow cytometry data showing the differentiation patterns and TCF1 and TOX expression of CD8+ T cells from splenocytes of TT PD-1 KO mice stimulated with anti-CD3/CD28 from Day 0(steady state) to Day 3. The data illustrate the differentiation patterns and the changes in TCF1 alongside variations in TOX, CD62L, CD44, and PD-1 within CD4+ T cells. (E) Histogram data comparing the expression levels of TCF1 and TOX between Day 1 and Day 2 post-stimulation in CD4+ T cells from two reporter mouse (TT and TT PD-1 KO) models.

3.3. Expression analysis of TCF1 and TOX in myeloid cells from TT mice and the impact of PD-1 deficiency

To measure the expression and changes of TCF1 and TOX in myeloid cells, neutrophils, monocytes, dendritic cells, and macrophages from the spleens of TT mice were analyzed using the following gating strategy: Neutrophils (Ly6C+Ly6G+CD11b+), Monocytes (Ly6C+Ly6G-CD11b+), Dendritic cells (DC: I-A/E+CD11c+Ly6C-Ly6G-CD11b+), and Macrophages (MAC: F4/80+Ly6C-Ly6G-CD11b+) **(Figure 5A and B)**. Neither TCF1 nor TOX was expressed in any of the myeloid cell subsets. Additionally, PD-1 deficiency did not affect the distribution of myeloid cell subsets or the expression of TCF1 and TOX.

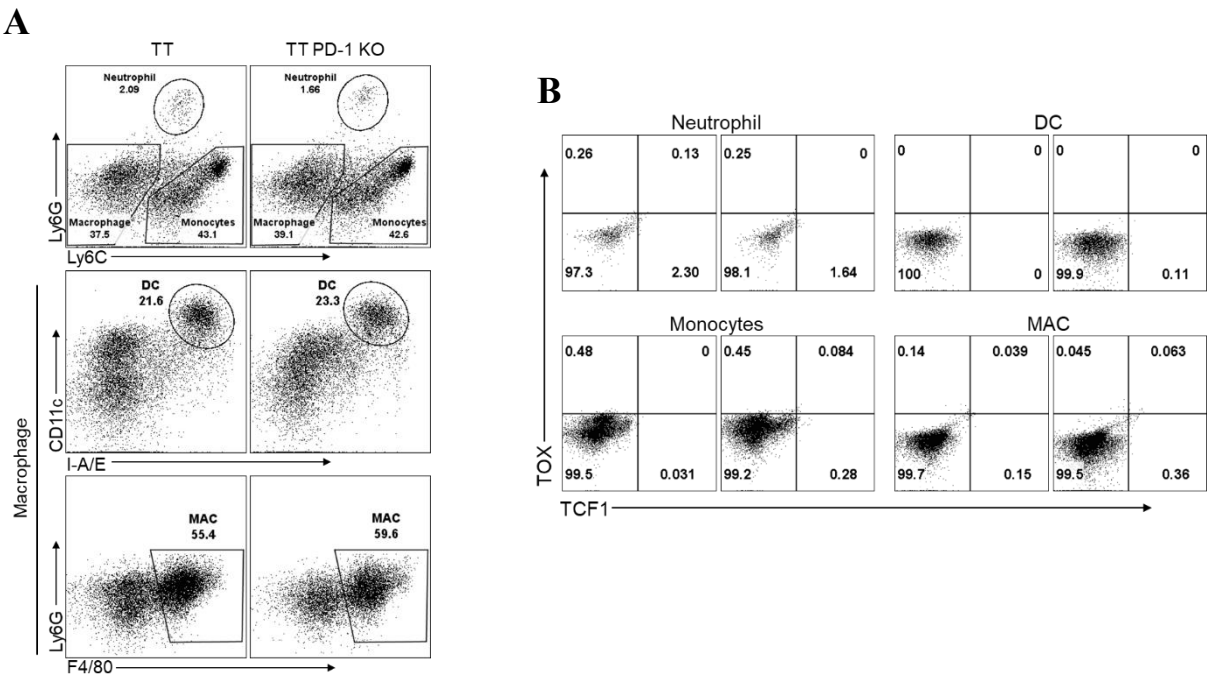

Figure 5 Myeloid cells don't express TCF1 and TOX

(A) To identify subsets of myeloid cells, excluding T cells and B cells. Briefly, T cells were identified by surface expression of CD3, and B cells were identified by surface expression of CD19. Myeloid cells were identified by surface expression of CD11b on CD3-CD19- cells. Subsequently, subsets of myeloid cells were distinguished. Neutrophils were identified as Ly6C+Ly6G+, and monocytes were identified

as Ly6C+Ly6G-. Within the Ly6C-Ly6G- population, dendritic cells (DCs) and macrophages (MACs) were distinguished. DCs were identified by surface expression of I-A/E and CD11c, while MACs were identified by surface expression of F4/80. In summary, the flow cytometric gating strategy for myeloid cell subsets: Neutrophils (Ly6C+Ly6G+CD11b+), Monocytes (Ly6C+Ly6G-CD11b+), Dendritic cells (DC: I-A/E+CD11c+Ly6C-Ly6G-CD11b+), and Macrophages (MAC: F4/80+Ly6C-Ly6G-CD11b+). (B) Flow cytometry data demonstrating the absence of TCF1 and TOX expression in subsets of myeloid cells.

3.4. Impact of enhanced tumor immunogenicity and PD-1 deficiency on tumor growth in mouse models

Cancer cells accumulate mutations, leading to genetic instability, altered protein expression, and unchecked growth. These mutations also increase their immunogenicity, enabling the immune system to recognize and eliminate them. To track the impact of tumor cell immunogenicity on CD8+ T cell differentiation through TCF1 and TOX expression, LLC1 lung carcinoma cells were engineered to express membrane-bound ovalbumin (OVA), increasing their immunogenicity. The OVA gene, in its membrane-anchored form, was inserted into a vector plasmid expressing GFP. Following the introduction of the mOVA gene into the LLC1 cell line, cells stably expressing this gene were selected based on GFP expression **(Figure 6A)**. Despite the overexpression of mOVA and GFP, the in vitro growth of LLC1 cells remained unaffected. LLC1 and LLC1-mOVA cells were then subcutaneously implanted into TT mice, and tumor growth was monitored **(Figure 6B)**. It was observed that TT mice receiving LLC1-mOVA experienced reduced tumor growth compared to those receiving WT LLC1, indicating that the increased immunogenicity of the tumor inhibited its growth **(Figure 6C)**. Subsequently, to explore the impact of PD-1 deficiency on in vivo tumor growth, LLC1 and LLC1-mOVA cells were implanted into PD-1 KO TT mice, and tumor growth was compared **(Figure 6B)**. LLC1 tumors exhibited a slight decrease in growth in PD-1 KO TT mice compared to WT TT mice. Interestingly, LLC1-mOVA tumors showed significantly reduced growth in PD-1 KO TT mice compared to WT TT mice **(Figure 6C and D)**.

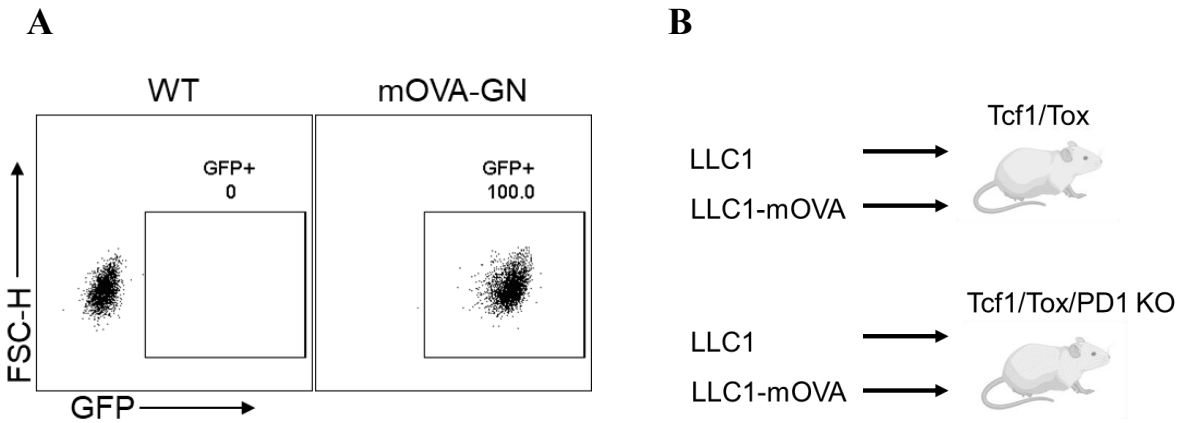

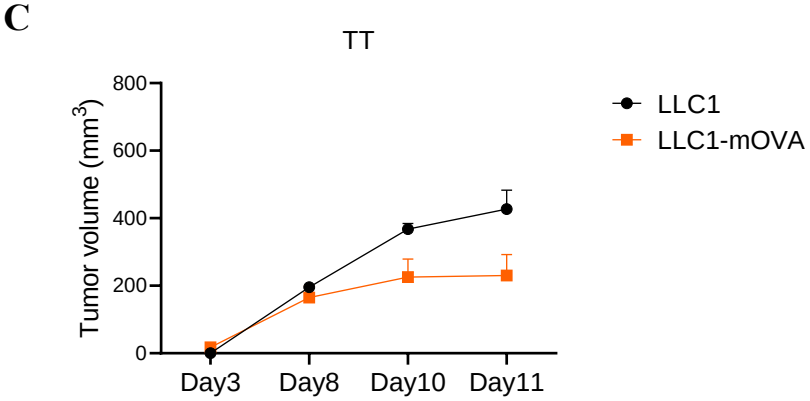

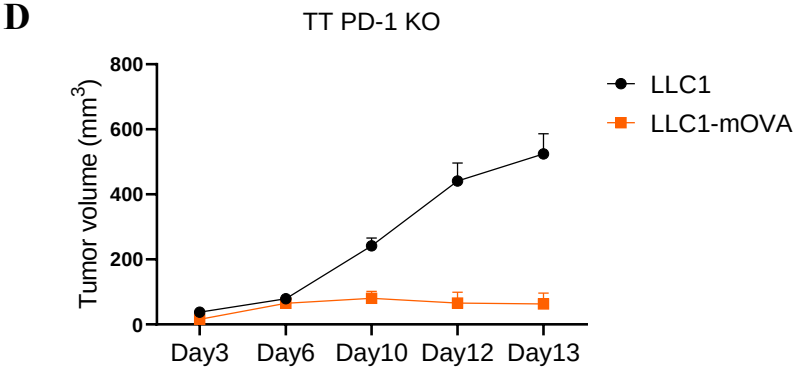

Figure 6 An increase in immunogenicity and PD-1 deficiency suppresses its growth

(A) The flow cytometry data confirming GFP expression in the generated LLC1-mOVA cell line. The DNA was cloned to ensure co-expression of GFP with mOVA, and then transfected into LLC1 cells. Subsequently, only the GFP+ population was sorted and cultured. (B) Experimental scheme for monitoring tumor growth and mouse analysis: 2.5×10^6 LLC1 or LLC1-mOVA cells were implanted into the flank of TT mice and TT PD-1 KO mice. (C) Tumor growth graphs (mean ± SEM) representing tumor volume measured with calipers after subcutaneous injection of 2.5×10^6 LLC1 or LLC1-mOVA cells into the flank of TT mice.; n=4~5 mice per group. (D) Tumor growth graphs (mean ± SEM) representing tumor volume measured with calipers after subcutaneous injection of 2.5×10^6 LLC1 or LLC1-mOVA cells into the flank of TT PD-1 KO mice.; n=4~5 mice per group.

3.5. Differential expression of TCF1 and TOX in tumor-infiltrating CD8+ T cells: implications for PD-1 deficiency and tumor immunogenicity

To assess changes in the differentiation status of tumor-infiltrating CD8+ T cells through TCF1 and TOX expression, TILs were isolated from tumors in mice and analyzed for TCF1 and TOX expression. In TT mice with LLC1 tumors, over 50% of CD8+ TILs expressed TCF1 but not TOX, while in LLC1-mOVA tumors, there was a notable increase in CD8+ TILs expressing both TCF1 and TOX **(Figure 7A and B)**. When comparing TCF1 and TOX expression in CD8+ TILs from WT and PD-1 KO mice receiving LLC1 tumors, a slight increase in the TCF1+TOX+ population was observed in PD-1 deficient CD8+ TILs **(Figure 7A and B)**. Interestingly, in PD-1 KO TT mice, there was a significant increase in the proportion of TCF1-negative population among LLC1-mOVA CD8+ TILs, which was not observed even in TT mice with well-controlled LLC1-mOVA CD8+ TILs, indicating an effect of PD-1 deficiency **(Figure 7B)**. This increase in the TCF1-negative population was accompanied by an increase in the TOX-negative population, although the TCF1-negative, TOX-positive population also increased **(Figure 7B)**. Notably, LLC1 CD8+ TILs in the same PD-1 KO TT mice did not show a similar increase in the TCF1-negative population as seen in LLC1-mOVA CD8+ TILs **(Figure 7B)**, suggesting that the enrichment of the TCF1-negative population in PD-1 KO TT mouse LLC1-mOVA CD8+ TILs was influenced by PD-1 deficiency and the immune-favorable tumor microenvironment associated with tumor immunogenicity.

A

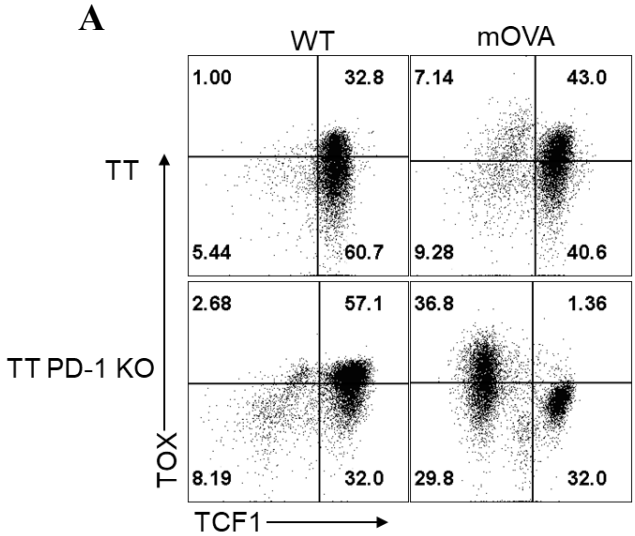

B

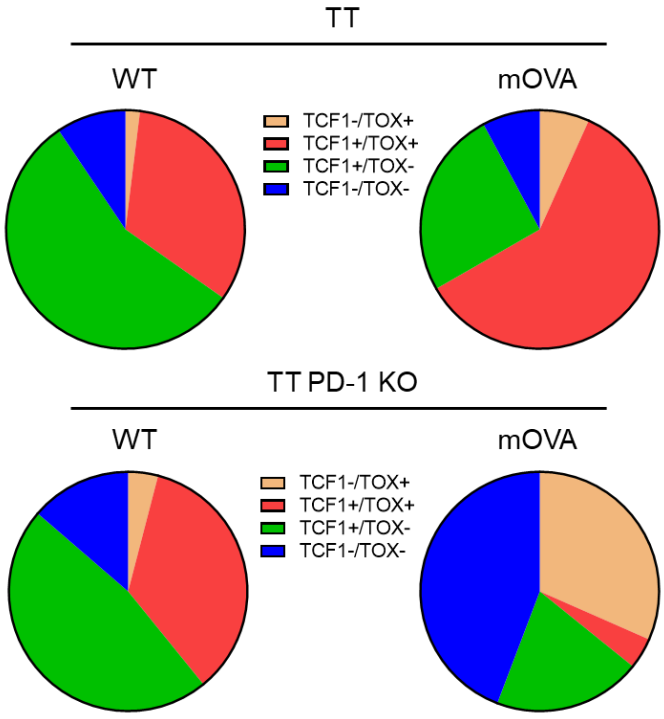

Figure 7 The change in the expression of TCF1 and TOX in CD8+ TILs is correlated with PD-1 deficiency and tumor immunogenicity

(A) The flow cytometric data showing the expression patterns of TCF1 and TOX in tumor-infiltrating CD8+ T cells from TT mice and TT PD-1 KO mice transplanted with LLC1 and LLC1-mOVA. Tumor tissue processing to obtain tumor-infiltrating T cells was performed between days 11 and 13 after subcutaneous implantation of LLC1 cell lines into TT mice and TT PD-1 KO mice. To distinguish between dead and live cells, NIR staining was conducted followed by Fc blocking to prevent nonspecific binding of fluorescently labeled antibodies to the Fc region. Subsequently, each target was stained with fluorochrome-conjugated antibodies. To identify tumor-infiltrating CD8+ T cells, live immune cells were gated first. The cells stained with NIR, indicative of cell death, were excluded, and gating was performed on cells expressing CD45, a prominent marker of immune cells. T cells were identified by surface expression of CD3, and CD8+ T cells were then distinguished. Subsequently, we monitored the expression of TCF1 and TOX. (B) Comparison graph of the percentages of tumor-infiltrating CD8+ T cell populations classified as TCF1-/TOX+, TCF1+/TOX+, TCF1-/TOX-, and TCF1+/TOX-. This data demonstrates that under conditions where increased tumor immunogenicity and PD-1 deficiency, the TCF1-negative population constitutes a larger proportion.

3.6. Impact of PD-1 expression and tumor immunogenicity on CD8+ TIL differentiation and immunophenotypic characteristics

To explore the relationship between PD-1 expression, tumor immunogenicity, and the differentiation dynamics of CD8+ T cells, an in-depth analysis was conducted on the immunophenotypic characteristics across four distinct subsets of CD8+ TILs, categorized based on their TCF1 and TOX expression. Initially, the expression of CD44, indicative of memory T cell differentiation, was observed in CD8+ TILs obtained from both LLC1 and LLC1-mOVA tumors implanted in TT mice as well as PD-1 KO TT mice. However, the variations emerged in the expression of CD62L, a marker linked to T cell memory and migration properties **(Figure 8A)**. Specifically, CD8+ TILs from TT mice harboring LLC1 tumors displayed the highest levels of CD62L expression, contrasting with a more moderate CD62L expression observed in approximately 50% of CD8+ TILs from both LLC1-mOVA bearing TT mice and PD-1 KO TT mice with LLC1 tumors. Conversely, a marked reduction in CD62L expression was evident in CD8+ TILs from PD-1 KO TT mice implanted with LLC1-mOVA tumors, where only around 10% of the population exhibited CD62L expression **(Figure 8B)**, suggesting a skew towards a Tem cell phenotype characterized by the CD62L-CD44+ signature **(Figure 8A)**. Additionally, CD62L expression was predominantly confined to the TCF1+ population within the CD8+ TILs **(Figure 8B)**. Furthermore, upon examining the expression of Tim-3, a marker associated with terminally exhausted T cells (Tex) or effector-like transitory cells, Tim-3 expression was found exclusively in the TCF1-negative subset of CD8+ TILs from mice bearing LLC1-mOVA tumors **(Figure 8C and D)**. No discernible differences in Tim-3 expression levels were observed between the TCF1-TOX+ and TCF1-TOX- populations **(Figure 8D)**. Notably, both the expression level and frequency of Tim-3 were markedly elevated within the TCF1-negative population of PD-1 deficient CD8+ TILs **(Figure 8E and F)**, suggesting a potential link between PD-1 deficiency, TCF1 expression, and Tim-3 upregulation in the CD8+ TIL.

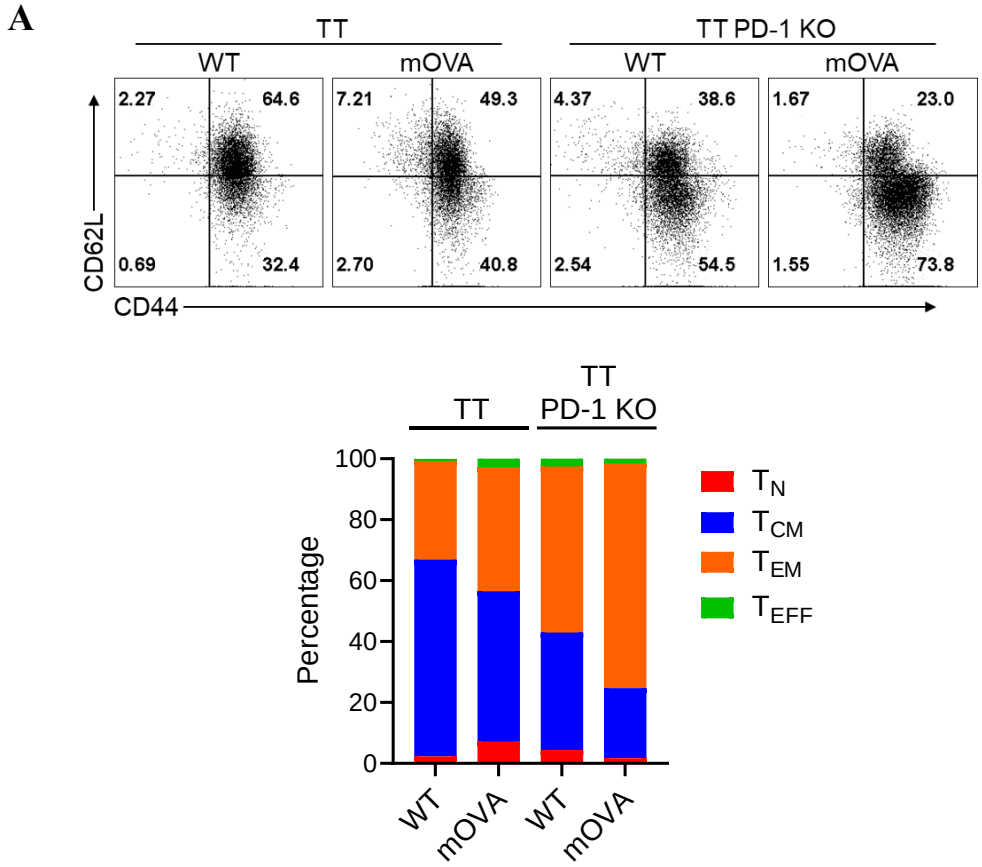

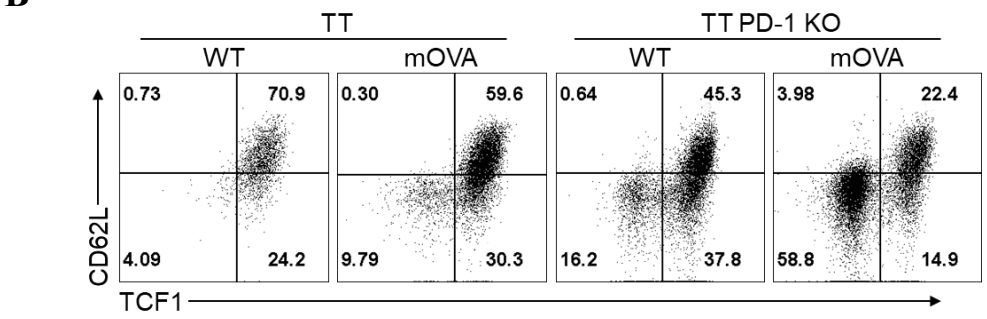

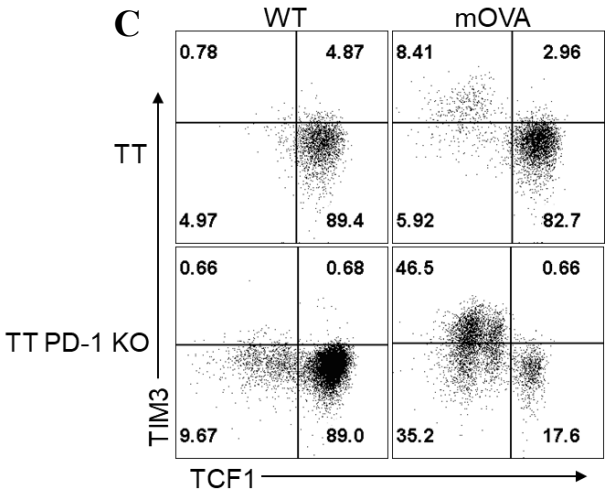

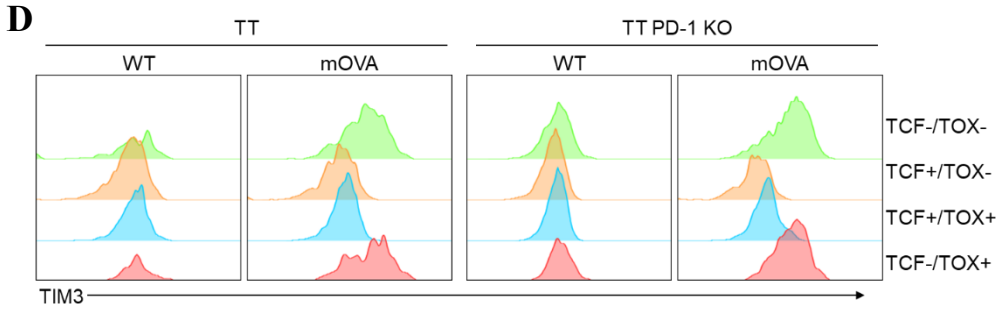

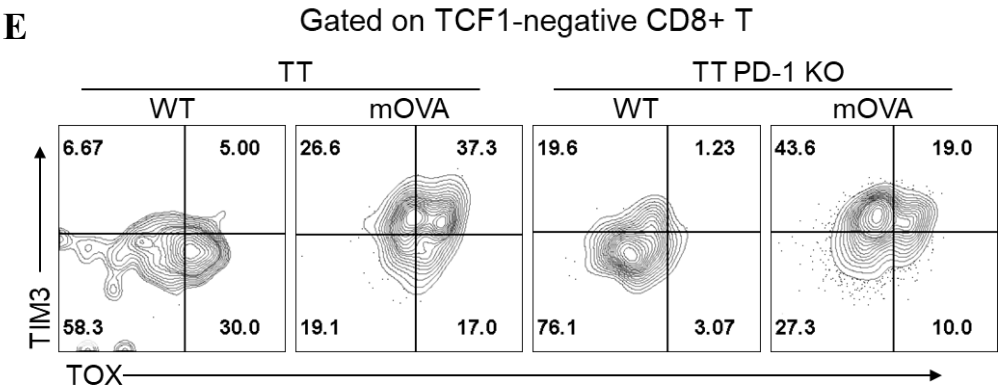

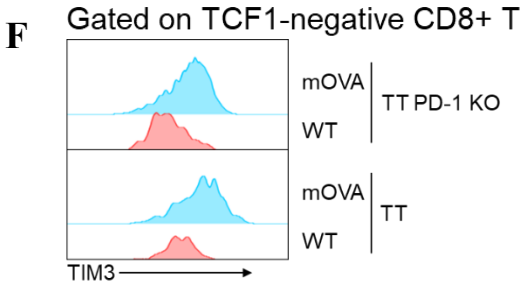

Figure 8 The change in TCF1 and TOX expression related to CD8+ TIL differentiation status

(A-F) Tumor tissue processing was performed between days 11 and 13 after subcutaneous implantation of LLC1 and LLC1-mOVA into TT mice and TT PD-1 KO mice to obtain tumor-infiltrating T cells (n=4~5 mice per group). To distinguish between dead and live cells, NIR staining was conducted followed by Fc blocking to prevent nonspecific binding of fluorescently labeled antibodies to the Fc region. Subsequently, each target was stained with fluorochrome-conjugated antibodies. To identify tumor-infiltrating CD8+ T cells, live immune cells were gated first. The cells stained with NIR, indicative of cell death, were excluded, and gating was performed on cells expressing CD45, a prominent marker of immune cells. T cells were identified by surface expression of CD3, and CD8+ T cells were then distinguished. Subsequently, we monitored the expression of TCF1 and TOX along with various markers.

(A) The flow cytometry analysis data illustrate the differentiation status of CD8+ TIL from TT mice and TT PD-1 KO mice implanted LLC1 and LLC1-mOVA. Additionally, the graphs depict the percentage of each subset of CD8+ TILs differentiation. Tn cell phenotype characterized by the CD62L+CD44- signature, Tcm cell phenotype characterized by the CD62L+CD44+ signature, Tem cell phenotype characterized by the CD62L-CD44+ signature and Teff cell phenotype characterized by the CD62L-CD44- signature. (B, D) The flow cytometry analysis data illustrate the change of TCF1 expression along with CD62L expression or TIM3 expression in CD8+ TIL from TT mice and TT PD-1 KO mice implanted LLC1 and LLC1-mOVA. A marked reduction in CD62L expression or increase in TIM3 expression was evident in CD8+ TILs from PD-1 KO TT mice implanted with LLC1-mOVA tumors. (D) The histogram data showing the change of TCF and TOX in CD8+ TILs from TT mice and TT PD-1 KO mice implanted LLC1 and LLC1-mOVA. The data categorized based on their TCF1 and TOX expression along with TIM3 expression. (E) The flow cytometry data showing the changes in TOX expression along with TIM3 conducted on the TCF1-negative CD8+ TILs. (F) The histogram data comparing the expression levels of TIM3 in TCF1-negative CD8+T TILs between TT mice and TT PD-1 KO mice harboring LLC1 and LLC1-mOVA tumors.

3.7. Characterization of of TCF1-negative CD8+ TIL subsets influenced by PD-1 deficiency and tumor immunogenicity

To further understand the activation status of CD8+ TIL subsets, the expression of T cell costimulatory molecules 4-1BB and CD226 was measured. Both CD226 and 4-1BB expression were higher in the TCF1-negative population compared to the TCF1-positive population, with no correlation observed between TOX expression and the expression of 4-1BB or CD226 **(Figure 9A)**. In PD-1 KO TT mice bearing LLC1-mOVA tumors, the expression of 4-1BB and CD226 in CD8+ TILs significantly increased as TCF1 expression decreased **(Figure 9A and B)**. However, in PD-1 KO TT mice bearing LLC1 tumors, the same TCF1-negative population exhibited lower levels of 4-1BB and CD226 compared to the CD8+ TILs in PD-1 KO TT mice with LLC1-mOVA tumors **(Figure 9C)**. This indicates that, in addition to PD-1 deficiency, tumor immunogenicity can result in the formation of sub-populations within the TCF1-negative population with different phenotypic characteristics and functionalities.

Next, the functionality of each subset was assessed through the expression of granzyme B and Ki-67. Interestingly, CD8+ TILs from mice with LLC1 tumors showed similar levels of granzyme B and Ki-67 expression across all four subsets, regardless of PD-1 expression. In contrast, in CD8+ TILs from mice bearing LLC1-mOVA tumors, granzyme B and Ki-67 were significantly higher in the TCF1-negative population compared to the TCF1-positive population **(Figure 9D and E)**. Within the TCF1-negative population, the frequency of cells expressing granzyme B and Ki-67 increased in the TCF1-TOX- subset **(Figure 9F)**. The TCF1-TOX+ population, known to be terminally differentiated late dysfunctional cells, exhibited lower granzyme B and Ki-67 expression compared to the highly cytotoxic TCF1-TOX- effector-like transitory population **(Figure 9F)**. In CD8+ TILs from PD-1 KO mice bearing LLC1-mOVA tumors, the increase in the TCF1-negative population corresponded with a significant increase in granzyme B and Ki-67 expression compared to CD8+ TILs from TT mice with LLC1-mOVA tumors **(Figure 9D and E)**.

In conclusion, the TCF1-negative population in highly immunogenic tumor-infiltrating CD8+ T cells represents a subset with high anti-tumor activity. This population appears to be promoted by PD-1 deficiency.

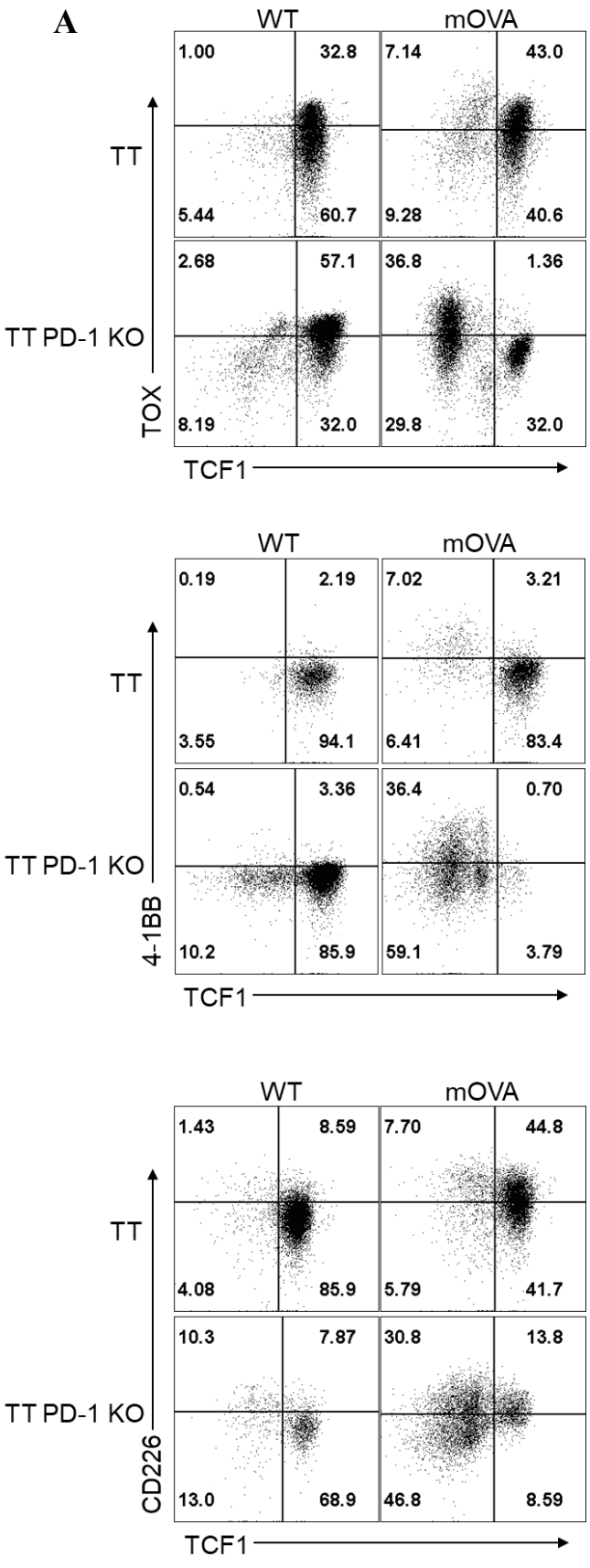

B

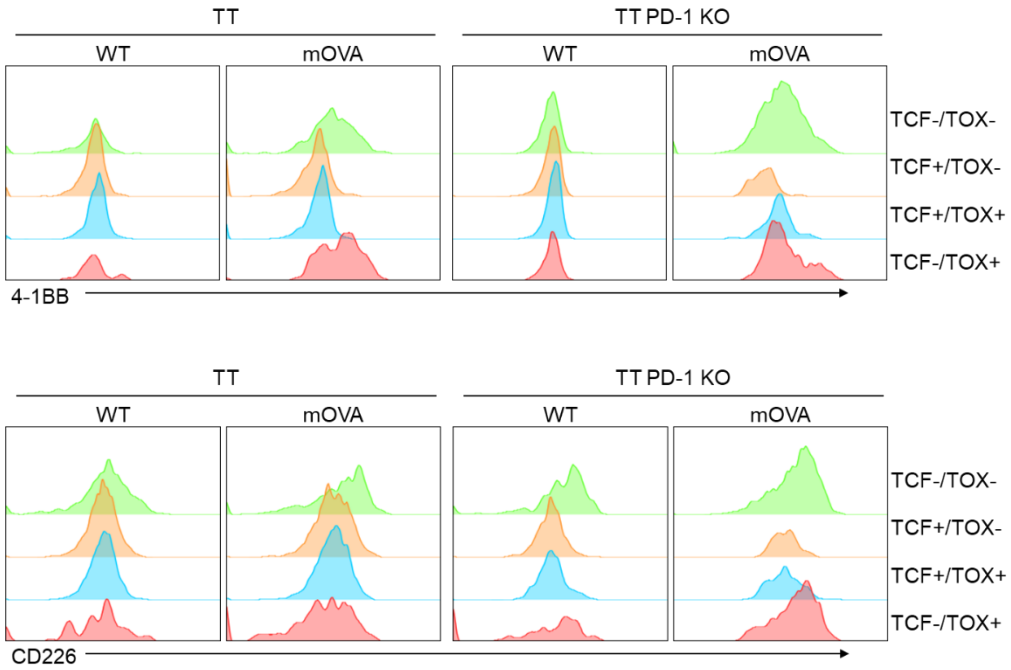

C

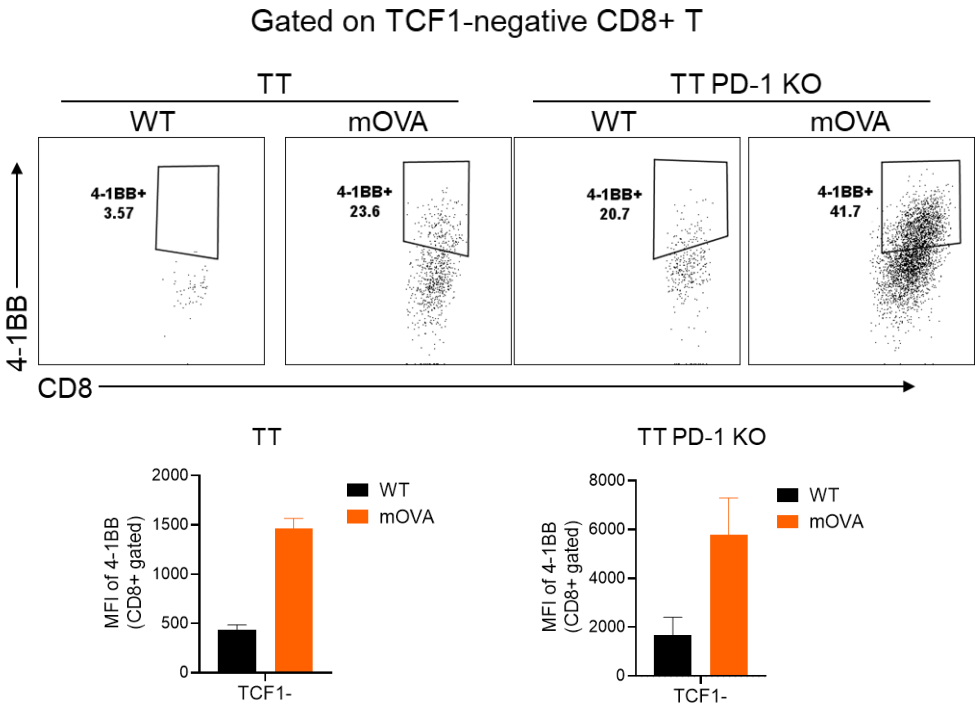

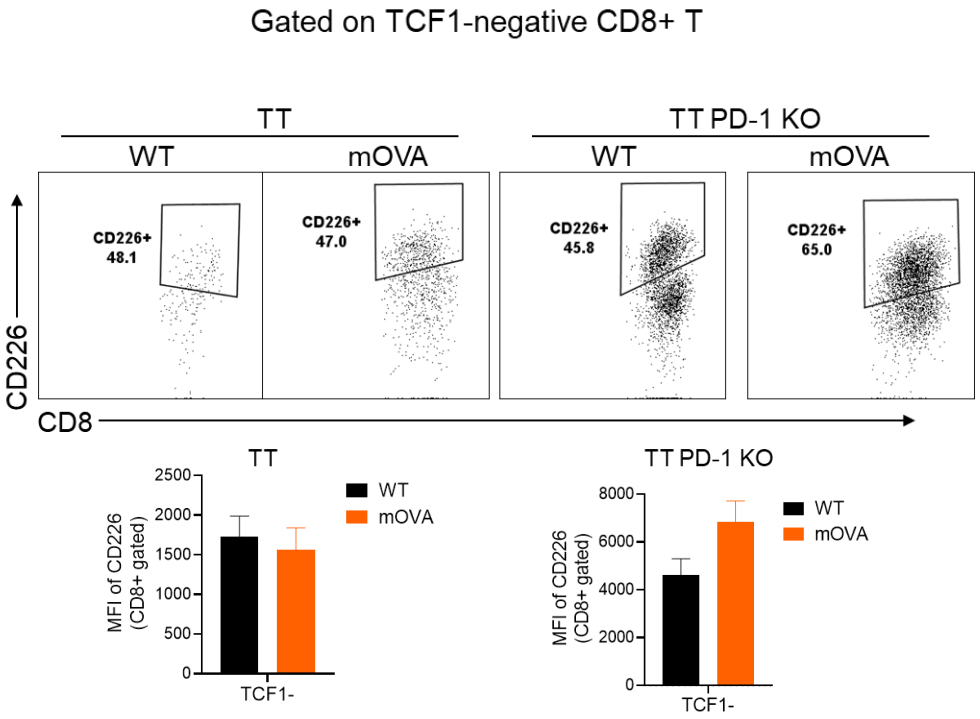

D

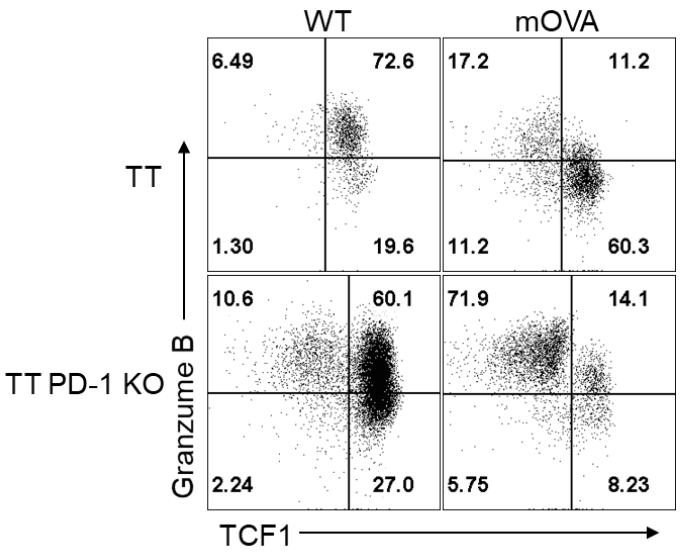

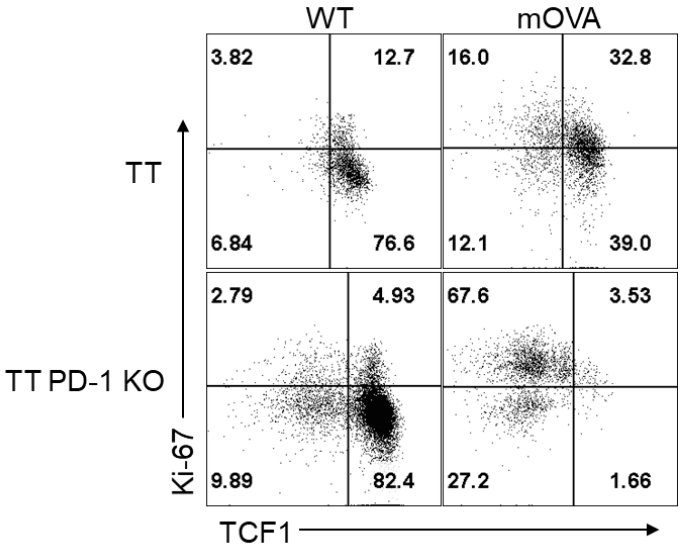

E

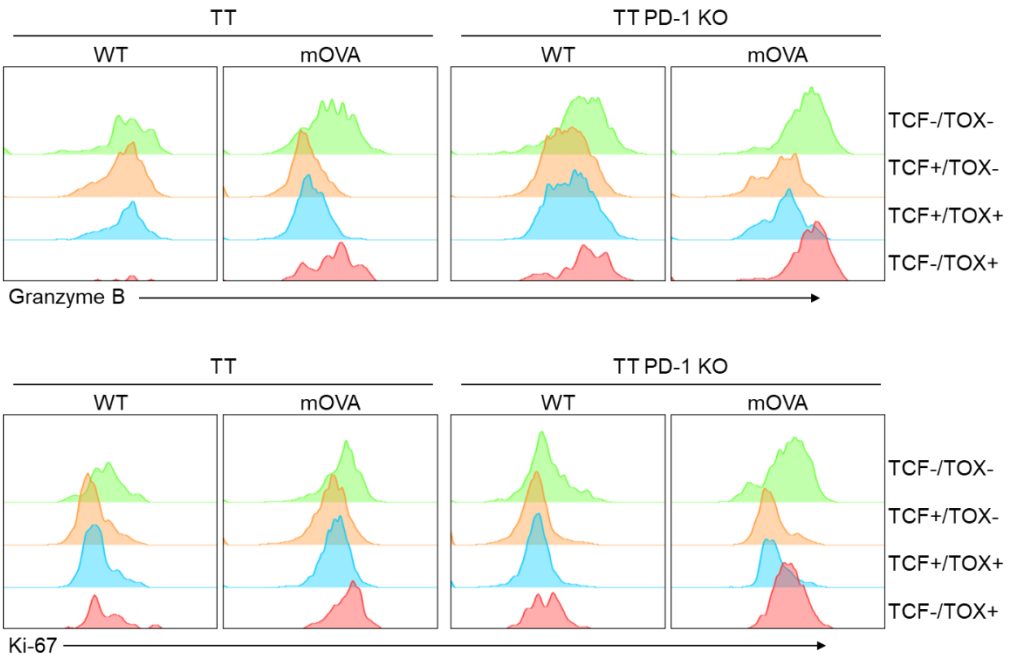

F

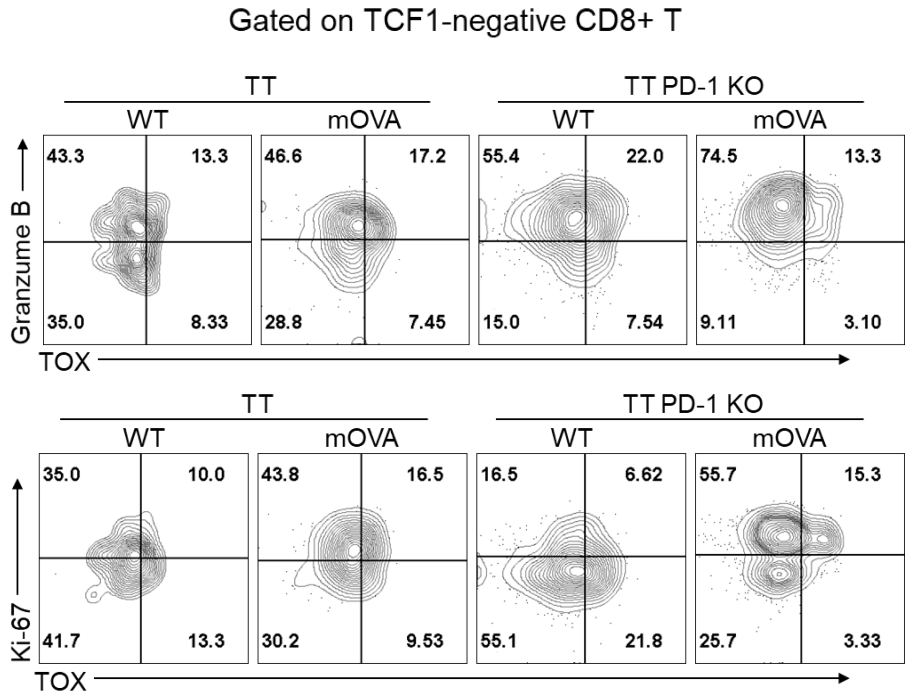

Figure 9 The TCF1-negative CD8+ T cells exhibit activated phenotypes in tumors

(A-F) Tumor tissue processing was performed between days 11 and 13 after subcutaneous implantation of LLC1 and LLC1-mOVA into TT mice and TT PD-1 KO mice to obtain tumor-infiltrating T cells (n=4~5 mice per group). To distinguish between dead and live cells, NIR staining was conducted followed by Fc blocking to prevent nonspecific binding of fluorescently labeled antibodies to the Fc region. Subsequently, each target was stained with fluorochrome-conjugated antibodies. To identify tumor-infiltrating CD8+ T cells, live immune cells were gated first. The cells stained with NIR, indicative of cell death, were excluded, and gating was performed on cells expressing CD45, a prominent marker of immune cells. T cells were identified by surface expression of CD3, and CD8+ T cells were then distinguished. Subsequently, we monitored the expression of TCF1 and TOX along with various markers.

(A) The flow cytometry analysis data illustrate the change of TCF expression along with TOX, 4-1BB and CD226 in CD8+ TIL from TT mice and TT PD-1 KO mice implanted LLC1 and LLC1-mOVA. (B) The histogram data showing the change of TCF and TOX in CD8+ TILs from TT mice and TT PD-1 KO mice implanted LLC1 and LLC1-mOVA. The data categorized based on their TCF1 and TOX expression along with 4-1BB expression and CD226 expression. As TCF1 expression decreased the expression of 4-1BB and CD226 in CD8+ TILs. (C) The flow cytometry analysis data showing the expression level of 4-1BB and CD226 gated on TCF1-negative CD8+ TILs from both reporter mouse. And the graph including the MFI of 4-1BB and CD226 gated on TCF1-negative CD8+ TILs. In the TCF1-negative population from PD-1 KO TT mice bearing LLC1 tumors, exhibited lower levels of 4-1BB and CD226. (D) The flow cytometry analysis data illustrate the change of TCF expression along with granzyme B and Ki-67 in CD8+ TIL from TT mice and TT PD-1 KO mice implanted LLC1 and LLC1-mOVA. (E) The histogram data showing the change of TCF and TOX in CD8+ TILs from TT mice and TT PD-1 KO mice implanted LLC1 and LLC1-mOVA. The data categorized based on their TCF1 and TOX expression along with granzyme B expression and Ki-67 expression. As TCF1-negative population in CD8+ TILs increased the expression of granzyme B and Ki-67. (F) The flow cytometry data showing the changes in TOX expression along with granzyme B and Ki-67 gated on the TCF1-negative CD8+ TILs. The expression of granzyme B and Ki-67 increased in the TCF1-TOX- subset.

4. Discussion

ICB therapy is a breakthrough in cancer treatment. However, it often does not provide lasting clinical benefits for many patients. This highlights the need to understand the cellular and molecular mechanisms behind ICB responses. In this context, a subset of CD8+ T cells has gained attention. These cells retain stemness and memory potential. They are emerging as crucial players in the response to ICB and other immune-based therapies. Intra-tumoral CD8+ stem-like T cells provide a proliferative burst. This burst seeds the effector response during ICB. TCF1 marks a downstream population of CD8+ stem-like precursors. These cells have high self-renewal capacity, proliferative potential, and polyfunctionality. They sustain the entire CD8+ T cell output. In vivo, they are mostly quiescent but retain high proliferative potential. TCF1 is expressed, though at lower levels, in a second subset of precursor cells. These cells express the PD-1 receptor and are highly proliferative at steady state. They give rise to downstream effector-like transitory cells. The transition from precursors to effector-like transitory cells involves TCF1 downregulation and T-bet upregulation. T-bet antagonizes TOX-mediated induction of a late dysfunctional phenotype in transitory effector-like T cells. These cells expand during ICB and contribute to tumor control. Ultimately, these T cells convert into late-dysfunctional T cells. These late-dysfunctional T cells express high levels of immune checkpoint receptors. They lack proliferative capacity, display low polyfunctionality, but retain killing capability. Late dysfunctional T cells increase TOX expression. One clinical study in melanoma patients supports the relevance of TCF1+ CD8+ stem-like T cells. This study showed that the frequency of TCF7-expressing CD8+ T cells correlated with a positive response to ICB [50].

However, in advanced clear cell renal carcinoma patients treated with ICB, the frequency of TCF1+ CD8+ T cells did not predict any clinical outcomes [51]. These findings suggest that the reliance on TCF1+ CD8+ stem-like T cells for ICB efficacy may not be consistent across patients or tumor types.

Recent mouse model studies have shed light on the interplay between tumor immunogenicity and the efficacy of ICB therapy. The study examined the correlation between responsiveness to ICB and TCF1 expression, as well as the relationship with immunogenicity. This analysis was conducted using both the highly immunogenic MC38-OVA tumor model and the low immunogenic B16-OVA tumor model [52]. In tumors with high immunogenicity, despite TCF1 deficiency causing the destabilization of intra-tumoral CD8+ T cells, there was an observed increase in the generation of short-lived effector CD8+ T cells. This increase facilitated tumor control by ICB. However, in low immunogenic cancers, the

presence or absence of the TCF1+ precursor CD8+ T cell population emerged as a critical determinant of the response to ICB. These findings highlight the complex relationship between tumor immunogenicity, TCF1 expression, and the efficacy of ICB, emphasizing the need for further investigation to optimize immunotherapeutic strategies.

To examine the factors influencing the differentiation of CD8+ TILs within tumors, I analyzed the changes in TCF1 and TOX expression dynamics in response to antigenicity, a critical determinant of cancer immunogenicity. Partial tumor control was observed in TT mice transplanted with LLC-mOVA cancer, accompanied by a significant increase in the population of TCF1 and TOX double-positive cells among CD8+ TILs compared to those infiltrating LLC1 cancer. Moreover, it is presumed that the TCF1+TOX- population, which dominates among CD8+ TILs within LLC1 cancer, reflects a naïve-like status, possibly attributed to the low level of antigen expression. In situations where cancer antigenicity remains unaltered, inhibiting PD-1, a pivotal factor impeding cancer immunogenicity, did not yield significant disparities in tumor control or in the dynamics of TCF1 and TOX expression when compared to WT TT mice. These results demonstrate, through the tracking of TCF1 and TOX expression dynamics, that T cell priming by antigen is a prerequisite for tumor control via immune checkpoint inhibition. When both an increase in cancer antigenicity and PD-1 deficiency in immune cells are present simultaneously, notable differences were observed not only in tumor control but also in the expression of TCF1 and TOX in tumor-infiltrating T cells. Specifically, in a comparison between CD8+ TILs from TT mice transplanted with LLC1-mOVA and CD8+ TILs from TT PD-1 KO mice with LLC1-mOVA, it was found that in PD-1 KO mice with LLC1-mOVA, the majority of CD8+ TILs consisted of a TCF1-negative population undergoing progressive differentiation. This indicates a significant shift toward effector-like transitory cells, characterized by the TCF1-TOX+ population. The expression of Tim-3, 4-1BB, CD226, and granzyme B also significantly increased in the TCF1-negative population of CD8+ TILs. The expression levels of these markers were higher in the TCF1-TOX- population compared to the TCF1-TOX+ late dysfunctional population. Interestingly, Ki-67 expression was also higher in the TCF1- population compared to the TCF1+ population. These findings suggest that the TCF1- population is activated by antigen and possesses effector functions, rather than exhibiting proliferative capacity due to self-renewal. Additionally, regardless of PD-1 expression in immune cells, increased tumor antigenicity led to higher expression of Tim-3, CD226, 4-1BB, granzyme B, and Ki-67 in the TCF1-negative population. This suggests that in antigen-primed CD8+ TILs, TCF1 downregulation is accompanied by progressive differentiation. In the same TCF1-negative population, when PD-1 is not expressed, there is higher expression of effector molecules like granzyme B. This

indicates that even under the same antigen priming conditions, the inhibition of PD-1 enhances the quality of priming. In other words, T cell priming is determined by the presence of antigens, and the quality and quantity of primed T cells are regulated by the presence of inhibitory immune checkpoint receptors such as PD-1. It is known that the dynamic differentiation and status of tumor-infiltrating CD8+ cells are key factors determining the success of ICB therapy.

However, due to the lack of specific surface markers that can be used to track the subsets of subdivided CD8+ TILs, monitoring the dynamic expression changes of TCF1 and TOX becomes essential for identifying the heterogeneous subsets of tumor-infiltrating CD8+ T cells. Without such markers, it is challenging to pinpoint the identity and function of these subsets accurately. To address this issue, this study employed a reporter mouse model designed to visualize TCF1 and TOX expression through fluorescence. This innovative approach allowed for precise tracking of the dynamic changes in TCF1 and TOX expression in response to varying levels of tumor immunogenicity. Through this method, it was possible to observe and measure how TCF1 and TOX expression patterns evolve, providing insights into the differentiation pathways and functional states of CD8+ TILs within the tumor microenvironment. By correlating these expression dynamics with the immunogenic properties of the tumor, the study was able to elucidate the intricate relationship between the optimal priming and differentiation of CD8+ TILs and specific tumor factors. This comprehensive analysis not only sheds light on the underlying mechanisms that govern T cell responses in cancer but also highlights the potential for using TCF1 and TOX as markers to better understand and perhaps improve the efficacy of ICB therapy.

Reference

1. Beatty, G.L. and W.L. Gladney, *Immune Escape Mechanisms as a Guide for Cancer Immunotherapy.* Clinical Cancer Research, 2015. **21**(4): p. 687-692.

2. Escors, D., *Tumour Immunogenicity, Antigen Presentation, and Immunological Barriers in Cancer Immunotherapy.* New Journal of Science, 2014. **2014**: p. 734515.

3. Kumar, A.R., et al., *Harnessing the immune system against cancer: current immunotherapy approaches and therapeutic targets.* Mol Biol Rep, 2021. **48**(12): p. 8075-8095.

4. Zhou, W.T. and W.L. Jin, *B7-H3/CD276: An Emerging Cancer Immunotherapy.* Front Immunol, 2021. **12**: p. 701006.

5. Meiliana, A., N.M. Dewi, and A.Y. Wijaya, *Cancer Immunotherapy: A Review.* The Indonesian Biomedical Journal, 2016. **8**: p. 1-20.

6. Darrow, T.L., C.L. Slingluff, Jr, and H.F. Seigler, *The role of HLA class I antigens in recognition of melanoma cells by tumor-specific cytotoxic T lymphocytes. Evidence for shared tumor antigens.* The Journal of Immunology, 1989. **142**(9): p. 3329-3335.

7. Brichard, V., et al., *The tyrosinase gene codes for an antigen recognized by autologous cytolytic T lymphocytes on HLA-A2 melanomas.* Journal of Experimental Medicine, 1993. **178**(2): p. 489-495.

8. Tsang, K.Y., et al., *Generation of Human Cytotoxic T Cells Specific for Human Carcinoembryonic Antigen Epitopes From Patients Immunized With Recombinant Vaccinia-CEA Vaccine.* JNCI: Journal of the National Cancer Institute, 1995. **87**(13): p. 982-990.

9. Bremers, A.J., et al., *The use of Epstein-Barr virus-transformed B lymphocyte cell lines in a peptide-reconstitution assay: identification of CEA-related HLA-A*0301-restricted potential cytotoxic T-lymphocyte epitopes.* J Immunother Emphasis Tumor Immunol, 1995. **18**(2): p. 77-85.

10. Campos-Perez, J., et al., *DNA fusion vaccine designs to induce tumor-lytic CD8+ T-cell attack via the immunodominant cysteine-containing epitope of NY-ESO 1.* Int J Cancer, 2013. **133**(6): p. 1400-7.

11. Kawakami, Y., et al., *Identification of a human melanoma antigen recognized by tumor-infiltrating lymphocytes associated with in vivo tumor rejection.* Proceedings of the National Academy of Sciences, 1994. **91**(14): p. 6458-6462.

12. Kawakami, Y., et al., *Identification of the immunodominant peptides of the MART-1 human melanoma antigen recognized by the majority of HLA-A2-restricted tumor infiltrating lymphocytes.* Journal of Experimental Medicine, 1994. **180**(1): p. 347-352.

13. Goldberger, Z., et al., *Membrane-localized neoantigens predict the efficacy of cancer immunotherapy.* Cell Reports Medicine, 2023. **4**(8): p. 101145.

14. Liechtenstein, T., et al., *Modulating Co-Stimulation During Antigen Presentation to Enhance Cancer Immunotherapy.* Immunology, Endocrine & Metabolic Agents in Medicinal Chemistry (Discontinued), 2012. **12**(3): p. 224-235.

15. Nurieva, R., et al., *T-cell tolerance or function is determined by combinatorial costimulatory signals.* The EMBO Journal, 2006. **25**(11): p. 2623-2633.

16. Liechtenstein, T., et al., *PD-L1/PD-1 Co-Stimulation, a Brake for T cell Activation and a T cell Differentiation Signal.* J Clin Cell Immunol, 2012. **S12**.

17. Lagos, G.G., B. Izar, and N.A. Rizvi, *Beyond Tumor PD-L1: Emerging Genomic Biomarkers for Checkpoint Inhibitor Immunotherapy.* American Society of Clinical Oncology Educational Book, 2020(40): p. e47-e57.

18. Albini, A., et al., *Contribution to Tumor Angiogenesis From Innate Immune Cells Within the Tumor Microenvironment: Implications for Immunotherapy.* Front Immunol, 2018. **9**: p. 527.

19. Fife, B.T. and K.E. Pauken, *The role of the PD-1 pathway in autoimmunity and peripheral tolerance.* Ann N Y Acad Sci, 2011. **1217**: p. 45-59.

20. Francisco, L.M., P.T. Sage, and A.H. Sharpe, *The PD-1 pathway in tolerance and autoimmunity.* Immunol Rev, 2010. **236**: p. 219-42.

21. Dong, H., et al., *Tumor-associated B7-H1 promotes T-cell apoptosis: a potential mechanism of immune evasion.* Nat Med, 2002. **8**(8): p. 793-800.

22. Rangel-Sosa, M.M., E. Aguilar-Córdova, and A. Rojas-Martínez, *Immunotherapy and gene therapy as novel treatments for cancer.* Colomb Med (Cali), 2017. **48**(3): p. 138-147.

23. Blank, C., T.F. Gajewski, and A. Mackensen, *Interaction of PD-L1 on tumor cells with PD-1 on tumor-specific T cells as a mechanism of immune evasion: implications for tumor immunotherapy.* Cancer Immunology, Immunotherapy, 2005. **54**(4): p. 307-314.

24. Nishimura, H., et al., *Immunological studies on PD-1 deficient mice: implication of PD-1 as a negative regulator for B cell responses.* International Immunology, 1998. **10**(10): p. 1563-1572.

25. Nishimura, H., et al., *Development of Lupus-like Autoimmune Diseases by Disruption of the PD-1 Gene Encoding an ITIM Motif-Carrying Immunoreceptor.* Immunity, 1999. **11**(2): p. 141-151.

26. Nishimura, H., et al., *Autoimmune dilated cardiomyopathy in PD-1 receptor-deficient mice.* Science, 2001. **291**(5502): p. 319-22.

27. Chikuma, S., *Basics of PD-1 in self-tolerance, infection, and cancer immunity.* Int J Clin Oncol, 2016. **21**(3): p. 448-55.

28. Speiser, D.E., et al., *T cell differentiation in chronic infection and cancer: functional adaptation or exhaustion?* Nat Rev Immunol, 2014. **14**(11): p. 768-74.

29. Blank, C.U., et al., *Defining 'T cell exhaustion'.* Nat Rev Immunol, 2019. **19**(11): p. 665-674.

30. Wherry, E.J., *T cell exhaustion.* Nature Immunology, 2011. **12**(6): p. 492-499.

31. McLane, L.M., M.S. Abdel-Hakeem, and E.J. Wherry, *CD8 T Cell Exhaustion During Chronic Viral Infection and Cancer.* Annu Rev Immunol, 2019. **37**: p. 457-495.

32. Saeidi, A., et al., *T-Cell Exhaustion in Chronic Infections: Reversing the State of Exhaustion and Reinvigorating Optimal Protective Immune Responses.* Frontiers in Immunology, 2018. **9**.

33. Sekine, T., et al., *TOX is expressed by exhausted and polyfunctional human effector memory CD8(+) T cells.* Sci Immunol, 2020. **5**(49).

34. Zhang, J., et al., *Role of TCF in differentiation, exhaustion, and memory of CD8(+) T cells: A review.* Faseb j, 2021. **35**(5): p. e21549.

35. Chen, Z., et al., *TCF-Centered Transcriptional Network Drives an Effector versus Exhausted CD8 T Cell-Fate Decision.* Immunity, 2019. **51**(5): p. 840-855.e5.

36. Jadhav, R.R., et al., *Epigenetic signature of PD-1+ TCF1+ CD8 T cells that act as resource cells during chronic viral infection and respond to PD-1 blockade.* Proceedings of the National Academy of Sciences, 2019. **116**(28): p. 14113-14118.

37. Zhou, X., et al., *Differentiation and persistence of memory CD8(+) T cells depend on T cell factor 1.* Immunity, 2010. **33**(2): p. 229-40.

38. Utzschneider, D.T., et al., *T Cell Factor 1-Expressing Memory-like CD8+ T Cells Sustain the Immune Response to Chronic Viral Infections.* Immunity, 2016. **45**(2): p. 415-427.

39. Utzschneider, D.T., et al., *T cells maintain an exhausted phenotype after antigen withdrawal and population reexpansion.* Nature Immunology, 2013. **14**(6): p. 603-610.

40. Im, S.J., et al., *Defining CD8+ T cells that provide the proliferative burst after PD-1 therapy.* Nature, 2016. **537**(7620): p. 417-421.

41. Miller, B.C., et al., *Subsets of exhausted CD8+ T cells differentially mediate tumor control and respond to checkpoint blockade.* Nature Immunology, 2019. **20**(3): p. 326-336.

42. Siddiqui, I., et al., *Intratumoral TCF1+PD-1+CD8+ T Cells with Stem-like Properties Promote Tumor Control in Response to Vaccination and Checkpoint Blockade Immunotherapy.* Immunity, 2019. **50**(1): p. 195-211.e10.

43. Khan, O., et al., *TOX transcriptionally and epigenetically programs CD8(+) T cell exhaustion.* Nature, 2019. **571**(7764): p. 211-218.

44. Yang, R., et al., *Distinct epigenetic features of tumor-reactive CD8+ T cells in colorectal cancer patients revealed by genome-wide DNA methylation analysis.* Genome Biol, 2019. **21**(1): p. 2.

45. Scott, A.C., et al., *TOX is a critical regulator of tumour-specific T cell differentiation.* Nature, 2019. **571**(7764): p. 270-274.

46. Beltra, J.C., et al., *Developmental Relationships of Four Exhausted CD8(+) T Cell Subsets Reveals Underlying Transcriptional and Epigenetic Landscape Control Mechanisms.* Immunity, 2020. **52**(5): p. 825-841.e8.

47. Liang, C., et al., *TOX as a potential target for immunotherapy in lymphocytic malignancies.* Biomarker Research, 2021. **9**(1): p. 20.

48. Alfei, F., et al., *TOX reinforces the phenotype and longevity of exhausted T cells in chronic viral infection.* Nature, 2019. **571**(7764): p. 265-269.

49. Han, H.S., et al., *TOX-expressing terminally exhausted tumor-infiltrating CD8+ T cells are reinvigorated by co-blockade of PD-1 and TIGIT in bladder cancer.* Cancer Letters, 2021. **499**: p. 137-147.

50. Sade-Feldman, M., et al., *Defining T Cell States Associated with Response to Checkpoint Immunotherapy in Melanoma.* Cell, 2019. **176**(1-2): p. 404.

51. Ficial, M., et al., *Expression of T-Cell Exhaustion Molecules and Human Endogenous Retroviruses as Predictive Biomarkers for Response to Nivolumab in Metastatic Clear Cell Renal Cell Carcinoma.* Clinical Cancer Research, 2021. **27**(5): p. 1371-1380.

52. Escobar, G., et al., *Tumor immunogenicity dictates reliance on TCF1 in CD8+ T cells for response to immunotherapy.* Cancer Cell, 2023. **41**(9): p. 1662-1679.e7.

국문 요약

CD8+ T 세포는 만성 바이러스 감염과 암과 싸우는 데 필수적이다. 그러나 항원과 환경 신호에 지속적으로 노출되면 CD8+ T 세포는 기능이 떨어지거나 "피로" 상태에 빠질 수 있다. 이러한 피로를 예방하는 것은 효과적인 질병 통제에 중요하다. 면역 관문 억제(Immune Checkpoint Blockade, ICB) 요법은 이러한 기능 저하 세포의 수용체를 억제하여 항암 및 항바이러스 반응을 크게 향상시켰다. 그러나 많은 환자에게서 지속적인 임상적 혜택을 얻는 것은 여전히 어려운 상황이다. T 세포 피로와 ICB 반응의 세포 및 분자 기전을 이해하는 것이 중요하다. TCF1 에 의해 조절되는 stem-like CD8+ T 세포는 ICB 요법에 대한 반응에 필수적이다. 최근 여러 연구에서는 ICB 효능을 위해 TCF1+CD8+ T 세포에 대한 의존성은 다양한 종양 맥락에 따라 다를 수 있다고 주장한다. 전사 인자 TOX 는 T 세포 피로를 시작하고 유지하는 유전 프로그램을 조절한다.

종양 내 CD8+ T 세포의 분화 또는 피로에 영향을 미치는 요소를 탐구하기 위해, TCF1 과 TOX 의 발현 동태를 추적할 수 있는 새로운 형광 리포터 마우스를 사용하여 CD8+ T 세포에서 TCF1 과 TOX 의 발현 동태를 분석하였다. 또한 PD-1 결핍의 영향을 평가하기 위해 PD-1 발현이 없는 리포터 마우스를 만들었다. 이 리포터 마우스에 LLC1 과 LLC1-mOVA 종양을 이식하여 종양 성장과 종양 침윤 림프구(TIL)에서 TCF1 과 TOX 의 발현 수준을 조사하였다.

LLC-mOVA 를 이식한 리포터 마우스에서 부분적인 종양 제어가 관찰되었으며, 이는 LLC1 에 비해 TCF+ TOX+ CD8+ TIL 이 상당히 증가함을 확인했다. 이는 LLC1 내 TCF1+TOX- CD8+ TIL 은 낮은 항원 발현으로 인한 naive-like 상태를 반영함을 시사한다. 암 항원성을 변화시키지 않은 상황에서의 PD-1 억제는 종양 제어나 TCF1 및 TOX 발현 변화에 미미한 영향을 끼쳤다. 그러나 암 항원성이 증가하고 PD-1 결핍이 동시에 존재할 때 종양 제어 및 CD8+ TIL 의 분화에서 두드러진 차이가 관찰되었다. LLC1-mOVA 를 가진 PD-1 KO 마우스의 CD8+ TIL 은 TCF1- population 을 다수 보였다. 이는 effector-like transitory 세포로 점진적으로 분화되는 세포이며, TCF1-TOX+ 이다. TCF1-CD8+ TIL 에서 Tim-3, 4-1BB, CD226, 그리고 granzyme B 의 발현 수준이 상당히 증가했으며, TCF1-TOX+ late dysfunctional population 에 비해 TCF1-TOX- population 에서 더 높은 수준으로 관찰되었다.

이 연구는 리포터 마우스 모델을 사용하여 TCF1 과 TOX 의 발현을 시각화하고, 이러한 변화 양상을 종양 면역원성과 연관시키며, CD8+ TIL 의 항원에 의한 활성화, 분화 및 종양 요인 간의 최적의 관계를 설명함으로써 ICB 요법의 효능에 대한 이해를 향상시킬 수 있다.